In re Application of: Michal DANIELY et al
Serial No.: 10/771,440
Filed: February 5, 2004
Office Action Mailing Date: December 27, 2006

Examiner: Duffy, Bradley
Group Art Unit: 1643
Attorney Docket: 26003

REMARKS

Reconsideration of the above-identified application in view of the amendments above and the remarks following is respectfully requested.

Claims 1-71 are in this Application. Claims 1-36 have been withdrawn from consideration. Claims 37-48, 51-65 and 68-71 have been rejected under 35 U.S.C. § 102. Claims 37, 49-51, 54-55, 66-68 and 71 have been rejected under 35 U.S.C. § 103. Claims 37-71 have been rejected under 35 U.S.C. § 112, first paragraph. Claims 37-71 have been rejected under 35 U.S.C. § 112, second paragraph. Claims 37, 41-53 and 55, 58-71 have been amended herewith. Claims 38 and 56 have been cancelled. New claims 72 and 73 have been added.

Declaration

The Examiner states that the oath or Declaration is defective because it does not correctly identify the city of residence and the city of the post office address of each inventor. Specifically, the Examiner states that the city of residence and the city of the post office address for inventor Eran Kaplan are incomplete as several letters in the city name appear to be missing. An Application Data Sheet is being provided herewith to overcome the objection to the Declaration.

Specification

The Examiner has objected to the specification because of the informalities related to the term "abovementioned" which occurs on Page 9, line 27. The Examiner's objection is respectfully traversed.

Applicants point out that the term "abovementioned" is not a typographical error and is defined as "mentioned previously" (adj.) (see for example, the online dictionary at http://www.thefreedictionary.com/abovementioned, attached entry).

In re Application of: Michal DANIELY et al
Serial No.: 10/771,440
Filed: February 5, 2004
Office Action Mailing Date: December 27, 2006

Examiner: Duffy, Bradley
Group Art Unit: 1643
Attorney Docket: 26003

35 U.S.C. § 112, second paragraph rejections

The Examiner has rejected claims 37-71 under 35 U.S.C. 112, second paragraph, as being indefinite for failing to particularly point out and distinctly claim the subject matter which Applicants regard as the invention.

Specifically, the Examiner states that claims 37-71 are indefinite because claims 37 and 55 recite the limitation "sequentially and/or simultaneously". The Examiner's rejections are respectfully traversed. Claims 37 and 55 have been amended to remove the phrase "sequentially and/or simultaneously", thereby rendering moot the Examiner's rejection with respect to these claims.

The Examiner further states that claims 41-47 and 58-64 are indefinite because claims 41 and 58 recite that the two stains are selected "independently" from the group consisting of a morphological stain, an immunological stain, an activity stain, a cytogenetical stain, an in situ hybridization stain and a DNA stain. The Examiner states that it is unclear on what basis the two stains are selected from the group; does one randomly choose two of the stains, or is some other basis used; if a one type of stain is selected for the first stain, is that same type of stain a possible choice for the second type; the Examiner submits that the meets and bounds of the subject matter that Applicants regard as the invention cannot be ascertained, as it cannot be determined how the recitation is intended to further limit the subject matter that is the invention with the requisite degree of clarity and particularity to satisfy the requirement set forth under 35 U.S.C. 112, second paragraph, so as to permit the skilled artisan to know or determine infringing subject matter. The Examiner's rejections are respectfully traversed. Claims 41 and 58 have been amended herewith.

Applicants point out that each of the staining methods pertaining to claims 41 and 58 can be selected for performing the claimed invention and that the instant application provides ample guidance for selecting pairs of stains or staining methods from the staining methods pertaining to claims 41 and 58 [see for example, Page 11

(lines 2-19), Page 15 (line 13 – Page 20 (line 24) and the Examples section (Pages 25-34) of the instant application]. For example, as described in the instant application (Page 15, lines 14-18) one staining method can be a morphological staining such as a May-Grünwald-Giemsa, a Giemsa, a Papanicolau or Hematoxylin-Eosin (which can be visualized via light microscopy, bright field), whereas another staining method can be an immunological staining using a fluorescently labeled antibody (which can be visualized via fluorescent microscopy, dark filed). In addition, one staining method can be an immunological staining using a radiolabelled antibody (which can be visualized using light microscopy) whereas another staining can be a morphological staining such as DAPI (which can be visualized via fluorescent microscopy) (see Page 16, lines 19-26 of the instant application). Given the comprehensive description of pairs of staining methods it is Applicants strong opinion that the metes and bounds of the subject matter of the invention are ascertained.

Non-withstanding the above and in order to expedite prosecution of this case, Applicants have elected to remove the term "independently" from claims 41 and 58, to thereby overcome the Examiner's rejection with respect to these claims.

The Examiner has rejected claims 48-53 and 65-70 because they recite the limitation "a first stain" and "a second stain", however, claims 37 and 55 from which these claims depend do not recite any order of stains and it is unclear whether more than one "first stain" or more than one "second stain" is being contemplated. The Examiner's rejections are respectfully traversed.

Claims 48-53 and 65-70 have been amended to include the limitation of "one" and "another" staining methods according with Examiner's suggestion. Ample support for such claim amendments can be found in the instant application, see for example, Page 9.

In view of the above claim amendments, arguments and remarks Applicants believe to have overcome the 35 U.S.C. § 112, second paragraph rejections.

In re Application of: Michal DANIELY et al
Serial No.: 10/771,440
Filed: February 5, 2004
Office Action Mailing Date: December 27, 2006

Examiner: Duffy, Bradley
Group Art Unit: 1643
Attorney Docket: 26003

35 U.S.C. § 112,first paragraph rejections

The Examiner has rejected claims 37-71 under 35 U.S.C. 112, first paragraph, as failing to comply with the written description requirement. Specifically, the Examiner states that claims 37-71 are directed at methods of identifying transitional cell carcinoma cells or diagnosing bladder cancer using at least two members of a genus of "stains", however, the specification does not describe the structure of a sufficient number of species of the genus of "stains" or a sufficient number of species of any of the subgenera of morphological stains, immunological stains, activity stains, cytogenetical stain, in situ hybridization stains or DNA stains to reasonably convey to the skilled artisan that Applicant had possession of the claimed invention at the time the application was filed. The Examiner's rejections are respectfully traversed. Claims 37, 41-53, 55, 58-70, have been amended herewith.

Applicants point out that the various stains described in the instant application are well-known and accepted art terms describing the reagents used by various staining methods (e.g., immunological staining; activity staining; morphological staining; cytogentical staining; DNA staining; and *in situ* hybridization). See for example, US Appl. No. 20030152987 and Ortona E., et al., 1997 (enclosed herewith) for morphological stains; Ambros PF., et al., 2001 (enclosed herewith) for immunological stains; Ried and Collmer, 1985 (enclosed herewith) for activity stains; Onozawa M., et al., 2003 (enclosed herewith) for cytogenetic reagents; DiMaio JM., et al., 1995 (enclosed herewith) for *in situ* hybridization; and Motte PM., et al., 1991 (enclosed herewith) for DNA stains.

In addition, Applicants point out that the instant application provides sufficient written support for the stains and staining methods used by the present invention. See for example, Page 11, lines 23-24 of the instant application for morphological staining, Page 12, lines 3-4 of the instant application for immunological staining, Page 12, lines 25-28 of the instant application for activity staining, Page 13, lines 6-16 of the instant application for cytogenetic methods [e.g., G-banding, Q-banding, R-

banding, and C-banding, Page 13, lines 17-25 of the instant application for *in situ* hybridization and Page 14, lines 25-29 of the instant application for DNA staining.

Non-withstanding the above and in order to expedite prosecution of this case, claims 37, 41-53, 55 and 58-70 have been amended to recite "staining method" instead of "stain".

In view of the above claim amendments, arguments and remarks Applicants believe to have overcome the 35 U.S.C. § 112, first paragraph rejections.

35 U.S.C. § 102(a) Rejections

The Examiner has rejected claims 37-48, 51-65 and 68-71 under 35 U.S.C. 102(a) as being anticipated by Daniely et al (Annales de Genetique, 46:153, September 2003) as evidenced by Shimoni et al. [Leukemia, 16:1413-1418, August 2002), Skacel et al. (Anal. Quant. Cytol. Histol. 23(6): 381-387, December 2001]. The Examiner's rejections are respectfully traversed.

Applicants point out that since the priority of the instant application is from April 4th, 2003, the filing date of U.S. Provisional Application No. 60/459,992, the art of Daniely et al. (September 2003), which describes the use of two staining methods (*i.e.,* morphological and FISH) cannot anticipate the present invention as claimed. Thus, Daniely et al., either alone or with Shimoni et al., or Skacel et al., cannot anticipate or render obvious the claimed invention since it is published after the established priority of the claimed invention.

Attached is a declaration by the present inventors stating that they are the only inventors of the present application.

In view of the above arguments and remarks Applicants believe to have overcome the 35 U.S.C. § 102(a), rejections.

In re Application of: Michal DANIELY et al
Serial No.: 10/771,440
Filed: February 5, 2004
Office Action Mailing Date: December 27, 2006

Examiner: Duffy, Bradley
Group Art Unit: 1643
Attorney Docket: 26003

35 U.S.C. § 102(b) Rejections

The Examiner has rejected claims 37-48, 52-53, 55-65 and 69-70 under 35 U.S.C. 102(b) as being anticipated by Skacel et al. (Anal Quant. Histol. 23(6): 381-387, December 2001). Specifically, the Examiner states that Skacel et al. teach staining cells with DAPI (a DNA stain) and FISH and exposing them to two imaging modes to identify transitional cell carcinoma or diagnosing bladder cancer. The Examiner's rejections are respectfully traversed. Claims 37 and 55 have been amended.

Applicants point out that in contrast to Examiner's assertion, Skacel et al. teach staining the cells with FISH and DAPI and viewing them under one imaging mode (*i.e.*, dark modality using a fluorescence microscope; Page 384, left column, lines 23-25 in Skacel et al.) and not under two different imaging modes as claimed in claims 37 and 55 of the instant application.

Non-withstanding the above, and in order to better distinct the claimed invention from the art, Applicants have elected to amend claim 37 to recite:

"A method of identifying transitional cell carcinoma cells in a urine sample comprising:
(a) staining nucleated cells of the urine sample by at least two staining methods to thereby obtain stained nucleated cells,
(b) imaging said stained nucleated cells by at least two imaging modes, wherein one imaging mode of said at least two imaging modes being different from another imaging mode of said at least two imaging modes."
(Emphasis added)

Support for the claim amendment can be found, for example, on Page 10 (lines 30-33) – Page 11 (lines 1-19) of the instant application.

Claim 55 has been amended accordingly.

In view of the above claim amendments, arguments and remarks Applicants believe to have overcome the 35 U.S.C. § 102(b), rejections.

35 U.S.C. § 103(a) Rejections

The Examiner has rejected claims 37, 54, 55 and 71 under 35 U.S.C. 103(a) as being unpatentable over Skacel et al. (Anal. Quant Cytol. Histol. 23(6):381-387, December, 2001), in view of Daniely et al. (Annales de Genetique, 46: 153, September 2003). The Examiner's rejections are respectfully traversed.

Applicants point out that as stated hereinabove with respect to 102(a) Rejections, the priority of the instant application should be from April 4th, 2003, the filing date of U.S. Provisional Application No. 60/459,992, therefore, the art of Daniely et al. (September 2003) should not be regarded as "prior art". Accordingly, the art of Skacel et al. in view of Daniely et al. cannot be regarded as patentability destroying of the instant application.

The Examiner has further rejected claims 37, 49-51, 54-55, 66-68 and 71 under 35 U.S.C. 103(a) as being unpatentable over Skacel et al. (Anal. Quant Cytol. Histol. 23(6):381-387, December, 2001) in view of US Patent 6,418,236 (Ellis et al., July 9, 2002). Specifically, with respect to US Patent 6,418,236 the Examiner states that the reference teaches automated image analysis using a microscope capable of dual imaging to image cells stained with two stains. The Examiner's rejections are respectfully traversed. Claims 37 and 55 have been amended.

Applicants point out that in contrast to the Examiner's assertion, US Patent 6,418,236 discloses a method of analyzing a biological specimen that has been consecutively stained with hematoxylin-eosin (H/E) and immunohistochemistry (IHC) or *in situ* hybridization (ISH) methods on parallel (*i.e.*, different) tissue sections (Column 1, lines 60-65 of US Patent 6,418,236). Thus, analysis of the biological specimen according to US Patent 6,418,236 is performed by pairing stored images of the different tissue sections stained with H/E and immunohistochemistry (*i.e.*, two

different tissue sections) (Column 2, lines 10-15; Column 5, lines 37-40, of US Patent 6,418,236). In contrast, as mentioned hereinabove with respect to 102(b) rejections, the instant invention as now claimed teaches staining and imaging of the same cell (same nucleated cell of the urine sample) using two staining methods which are viewed by two different imaging modes.

Thus, it is Applicants strong opinion that the subject matter of the invention as now claimed in claims 37 and 55 is novel and non-obvious with respect to Skacel et al. and Ellis et al., either along or in combination.

The Examiner has further rejected claims 37, 49-50, 55 and 66-67 under 35 U.S.C. 103(a) as being unpatentable over Daniely et al. (Annals de Genetique, 46:153, September 2003) in view of US Patent 6,418,236 (Ellis et al., July 9, 2002).

Applicants point out that since as stated hereinabove with respect to 102(a) Rejections, the priority of the instant application should be from April 4th, 2003, the filing date of U.S. Provisional Application No. 60/459,992, the art of Daniely et al. (September 2003) should not be regarded as "prior art". Accordingly, Daniely et al could not be regarded as patentability destroying either alone or in combination with other art (Ellis et al.) since it is published after the established priority of the claimed invention.

In view of the above claim amendments, arguments and remarks Applicants believe to have overcome the 35 U.S.C. § 103(a), rejections.

The Examiner further states that the prior art of Halling et al. (Journal of Urology, 164:1768-1775, November 2000), Bubendorf et al. (Anatomic Pathology, 116:79-86, 2001) and Darzynkiewicz et al. (Experimental Cell Research, 249: 1-12, 1999) made of record and not relied upon is considered pertinent to Applicant's disclosure. Applicants concur with Examiner's assertion with respect to these art.

In re Application of: Michal DANIELY et al
Serial No.: 10/771,440
Filed: February 5, 2004
Office Action Mailing Date: December 27, 2006

Examiner: Duffy, Bradley
Group Art Unit: 1643
Attorney Docket: 26003

In view of the above amendments and remarks it is respectfully submitted that claims 37, 39-55, 57-71 are now in condition for allowance. A prompt notice of allowance is respectfully and earnestly solicited.

Respectfully submitted,

Martin D. Moynihan
Registration No. 40,338

Date: May 15, 2007

Encls:

- Two-month extension fee
- Executed Declaration
- Additional Claim Transmittal Sheet
- An Application Data Sheet is being provided herewith to overcome the objection to the Declaration.
- http://www.thefreedictionary.com/abovementioned, attached entry
- ***References:***
- US Pat. Appl. No. 20030152987;
- Ambros PF., et al., Leukemia, 2001, 15: 275-277;
- DiMaio JM., Circulation. 1995;92:202-205;
- Motte PM., et al., J. of Histochemistry and Cytochemistry, 1991, 39: 1495-1506;
- Onozawa M., et al., Cancer Genet. Cytogenet. 2003, 147: 134-9;
- Ortona E., et al., J. of Clin. Microbiology, 1997, 35:1589-1591;
- Ried JL and Collmer A. Applied and Environmental Microbiology, 50: 615-622.

Leukemia (2001) 15, 275–277

www.nature.com/leu

SYNOPSIS

Unequivocal identification of disseminated tumor cells in the bone marrow by combining immunological and genetic approaches – functional and prognostic information

The detection and quantification of disseminated tumor cells (DTC) present in the bone marrow (BM), peripheral blood (PB) and apheresis products (AP) are becoming increasingly significant in the treatment of cancer patients. Three different applications are implemented in the clinical practice of pediatric and adult solid tumor patients: (1) the identification of tumor cells in the BM and PB at diagnosis; (2) the response of occult tumor cells to high-dose chemotherapy; and (3) the presence of tumor cells in the autograft. In solid tumors the clinical significance of DTCs at diagnosis or during the course of the disease, usually termed minimal residual disease (MRD) testing, is still under debate. These indistinct results are mainly due to methodical reasons. Therefore, a fully automated system (*RC*Detect/metafer) combining the detection of 'tumor-specific' immunological features together with 'tumor-typical' DNA aberrations has been developed allowing the unambiguous visualization of tumor cells in a hematopoietic surrounding.

There is still an ongoing debate whether or not neuroblastoma (NB) patients with localized disease show disseminated tumor cells in the bone marrow (BM) at diagnosis. Moss and coworkers[1] observed tumor cell infiltrates in 34% of the stage I, II and III patients with immunocytochemical (ICC) approaches. They also found a correlation between the presence of DTCs and unfavorable outcome. PCR techniques also disclosed positive reactions in bone marrow samples from patients with localized disease.[2] Data generated with a fluorescence-based detection system identified only one out of 128 NB patients with localized/regional disease (stages 1, 2A, 2B and 3) with a genetically verified tumor cell infiltrate (Méhes *et al*, submitted).

Bone marrow involvement in patients with localized epithelial tumors, best studied in breast carcinoma (BC) patients, were found in the range of 23% to 82% using PCR approaches[3] or alkaline phosphatase-based cytokeratin (CK) detection for example.[4] So far, these results cannot be reproduced by using a fluorescence-based detection of CK combined with a genetic analysis of doubtful cells.[15,16] Despite the fact that BM samples from only 45 patients with stage 1 or 2 were analyzed, these data clearly indicate that DTC data have to be analyzed critically and quality control studies especially on methodical issues have to be undertaken in order to obtain comparable results.

The response testing to chemotherapy turned out to be of clinical relevance in pediatric ALL patients especially.[5] Also, in stage 4 neuroblastoma patients with genetically aggressive tumors, we observed that the delayed tumor cell clearance of the bone marrow indicated an unfavorable outcome. Rapid bone marrow clearance seems to be associated with a decreased risk of death (Ambros *et al* unpublished). However, the exact time points when to measure the response are still unknown. Whether this finding, which was made on a limited number of patients, holds true for larger groups of patients, and also the question of whether all genetic subtypes behave in the same way, awaits further studies.

Hematopoietic reconstitution with autologous cells after high-dose chemotherapy in the course of autologous stem cell transplantation for the treatment of solid tumor patients has highlighted the concerns about tumor cell contamination of the autograft. Indirect evidence that tumor cells are responsible for the post-transplant relapse are provided by Ref. 6. In addition, the presence of tumor cells in the autograft has been correlated with an unfavorable post-transplant outcome in neuroblastoma.[7]

A number of strategies allow the identification and estimation of the number of disseminated tumor cells in the hematopoietic system or blood products. Most methods are indirect approaches detecting either genes expressed predominantly or exclusively by tumor cells (eg tyrosine hydroxylase in neuroblastomas, cytokeratin in breast carcinomas) or m-RNAs from gene fusion products as a result of reciprocal translocations (eg bcr/abl in CML patients or *EWS/FLI1* in Ewing tumors).

Although the rearranged gene product can be detected by RT-PCR techniques at a high sensitivity, these methods have the disadvantage of false positive results most often caused by contamination. In addition, physiological differences in the expression level of a certain gene product can also obscure the picture. This is especially difficult when analyzing RNA molecules, which although predominantly expressed in the target cell, can also be expressed under certain circumstances by non-neoplastic cells; best exemplified are these false positive results in BM samples from healthy individuals. Here, the number of positive results reaches up to 100% of the samples tested.[8] Furthermore, translocation-specific gene products can also be influenced by physiological conditions or even application of certain drugs.[9]

Flow cytometric analyses of rare tumor cells rely on automatic detection of immunofluorescence-labeled antibodies. Besides the use of multiparameter analysis and the high speed of these assays, the sensitivity level is rarely below 1 target cell in 10^{-4} MNCs. In addition, non-tumor cells may stain unspecifically and cell morphology cannot be assessed. Only combinations with, for example, PCR techniques can verify the genetic make up of the target cells.[10]

Culture techniques for DTC detection are virtually the only assays that provide information on the viability and clonogenicity of rare tumor cells. Daxter-type and agarose-based clonogenic assays are in use.[11] The disadvantages are contamination problems, lack of tumor cell growth besides the presence of vital tumor cells, technical difficulties and time requirements, all of which render culture methods not feasible as a routine method.

Until recently, the direct visualization of tumor cells in the

Correspondence: PF Ambros; Fax: +43/1/4087230
Received 27 March 2000; accepted 19 October 2000

Figure 1 Three color immunofluorescence of breast carcinoma cell positive staining with cytokeratin (green) and mucin (red) in (a). Tumor-typical numerical chromosomal changes were demonstrated by FISH using chromosome-specific DNA probes. The tumor-typical aberrations: pentasomy of chromosome X (green) and disomy of chromosome 16 (red) are shown in (b); trisomy 21 (red) and disomy 12 (green), shown in (c), were demonstrated sequentially on the same cell after automatic relocation of the immunological positive cell, thus providing an ultimate proof of the neoplastic nature of the target cell.

microscope has been hampered by technical problems. Virtually all antibodies reacting with 'tumor-specific' antigens also react with hematopoietic or epidermal cells. Cytoplasmic cells that contain internalized tumor cell debris also react with the antibodies. Furthermore, the visualization of the antibody by enzymatic detection can cause false positive reactions especially for peroxidase-labeled second antibodies but also for alkaline phosphatase (AP). Double ICC staining recognized the majority of these cells reacting directly to AP as mature plasma cells,[12] thus giving false positive results which can obscure the picture, especially when minor cell fractions are AP-positive mimicking tumor cells. On the other hand, immunological approaches are fast, simple, cheap and very sensitive.

The detection of specific gene rearrangements resulting from tumor-typical translocations and other tumor-typical aberrations can be performed by FISH on the DNA level. Besides the high specificity of this method the high sensitivity needed for DTC detection can usually not be achieved.

To circumvent the lack of specificity inherent to ICC techniques, a combination of the immunolgical information with a second tumor-typical marker is essential. This can be achieved either by the introduction of a second or third immunological stain or, ideally, by a combination of an immunological procedure and the detection of a tumor-typical genetic aberration. The demonstration of both the immunological profile and the genetic information on the same cells achieves the high sensitivity of the first technique and the high specificity of FISH techniques. Basically, these two pieces of information can be monitored simultaneously or sequentially. Simultaneous approaches detecting changes on the DNA level and specific cell surface or intercellular antigens are difficult to undertake on a routine basis as these two technological approaches use different pretreatment conditions. On the other hand, a sequential demonstration of genetic aberrations and phenotypic information is difficult to perform on rare cells as it is virtually impossible to relocate these cells without any automatic relocation system. Recently, we were able to introduce an automatic system (*RC*Detect/metafer; MetaSystems, Altlussheim, Germany) which has been developed to sequentially identify different cell markers on rare tumor cells. Four major goals can be achieved using this automatic system: (1) a high sensitivity can be reached as demonstrated by spiking experiments performed with neuroblastoma cells and breast carcinoma cells. All cells intermixed with normal BM or PB cells could be recovered (Mehes *et al* in press). Thus we can conclude that: (1) the sensitivity of this method is restricted only by the number of cells available for analysis; (2) the specificity of the recognition system is given by the fact that additional features typical for the tumor cell – either immunological or, even better, genetic aberrations can be simultaneously and/or sequentially demonstrated; in addition, (3) a reliable and exact quantification of all cells (hematopoietic and tumor cells) is possible; and (4) multi-parameter analyses of different cell features, so far only restricted to flow cytometric methods, are possible and functional characterization of rare tumor cells can be studied (Ki-67, apoptosis-related molecules, or multi-drug resistance molecules). Besides the detection of tumor-typical immunostains such as GD2, CD99 and cytokeratin, leukemia-specific antigens CD34, CD19 etc the tumor/leukemia associated genetic aberrations can be identified by the use of FISH analysis as well. An example of a combined immunological and genetic visualization of a tumor cell is given in Figure 1. A breast carcinoma cell was characterized by a double color immunofluorescence staining with cytokeratin and mucin. After automatic relocation of the same cell a genetic visualization of the tumor typical genetic aberrations was undertaken.

One of the most crucial questions, detecting DTCs in the hematopoetic system is the analysis of their functional status. PCR approaches but also ICC methods cannot discriminate between intact and dead cells or cell fragments, possibly entrapped into phagocytic cells. Thus, studies should include tests on the proliferation capacity, expression of drug resistance-associated genes and occurrence of apoptosis. So far, only very limited information on the functional status of DTC exists. In BC patients it was demonstrated that DTCs show a dormant state of cell growth indicated by little Ki-67 expression.[13] Data on neuroblastoma patients on the other hand indicate that disseminated tumor cells show a relatively high Ki-67 expression with a median value of 30% in untreated tumor patients (Mehes unpublished) and this figure is in line with the Ki-67 expression found in untreated neuroblastic tumors.[14]

In summary, this new detection method allows an accurate diagnosis, exact quantification, and functional characterization of low tumor cell infiltrates in the hematopoietic system besides offering an ideal way to monitor the response of the tumor cells to cytotoxic treatment.

PF Ambros
G Méhes
C Hattinger
IM Ambros
A Luegmayr
R Ladenstein
H Gadner

CCRI, St Anna Kinderspital
Kinderspitalg. 6
A-1090 Vienna, Austria

References

1 Moss TJ, Reynolds CP, Sather HN, Romansky SG, Hammond GD, Seeger RC. Prognostic value of immunocytologic detection of bone marrow metastases in neuroblastoma. *New Engl J Med* 1991; **324**: 219–226.
2 Cheung IY, Barber D, Cheung NK. Detection of microscopic neuroblastoma in marrow by histology, immunocytology, and reverse transcription-PCR of multiple molecular markers. *Clin Cancer Res* 1998; **4**: 2801–2805.
3 Vannucchi AM, Bosi A, Glinz S, Pacini P, Linari S, Saccardi R, Alterini R, Rigacci L, Guidi S, Lombardini L, Longo G, Mariani MP, Rossi-Ferrini P. Evaluation of breast tumour cell contamination in the bone marrow and leukapheresis collections by RT-PCR for cytokeratin-19 mRNA. *Br J Haematol* 1998; **103**: 610–617.
4 Braun S, Pantel K, Muller P, Janni W, Hepp F, Kentenich CR, Gastroph S, Wischnik A, Dimpfl T, Kindermann G, Riethmuller G, Schlimok G. Cytokeratin-positive cells in the bone marrow and survival of patients with stage I, II, or III breast cancer (see comments). *New Engl J Med* 2000 **342**: 525–533.
5 van Dongen JJ, Seriu T, Panzer-Grumayer ER, Biondi A, Pongers-Willemse MJ, Corral L, Stolz F, Schrappe M, Masera G, Kamps WA, Gadner H, van Wering ER, Ludwig WD, Basso G, de Bruijn MA, Cazzaniga G, Hettinger K, van der Does-van den Berg A, Hop WC, Riehm H, Bartram CR. Prognostic value of minimal residual disease in acute lymphoblastic leukaemia in childhood (see comments). *Lancet* 1998; **352**: 1731–1738.
6 Brenner MK, Rill DR, Holladay MS, Heslop HE, Moen RC, Buschle M, Krance RA, Santana VM, Anderson WF, Ihle JN. Gene marking to determine whether autologous marrow infusion restores long-term haemopoiesis in cancer patients. *Lancet* 1993; **342**: 1134–1137.
7 Lode HN, Handgretinger R, Schuermann U, Seitz G, Klingebiel T, Niethammer D, Beck J. Detection of neuroblastoma cells in CD34+ selected peripheral stem cells using a combination of tyrosine hydroxylase nested RT-PCR and anti-ganglioside GD2 immunocytochemistry. *Eur J Cancer* 1997; **33**: 2024–2030.
8 Dent GA, Civalier CJ, Brecher ME, Bentley SA. MUC1 expression in hematopoietic tissues. *Am J Clin Pathol* 1999; **111**: 741–747.
9 Pane F, Mostarda I, Selleri C, Salzano R, Raiola AM, Luciano L, Saglio G, Rotoli B, Salvatore F. BCR/ABL mRNA and the P210(BCR/ABL) protein are downmodulated by interferon-alpha in chronic myeloid leukemia patients. *Blood* 1999; **94**: 2200–2207.
10 Neale GA, Coustan-Smith E, Pan Q, Chen X, Gruhn B, Stow P, Behm FG, Pui CH, Campana D. Tandem application of flow cytometry and polymerase chain reaction for comprehensive detection of minimal residual disease in childhood acute lymphoblastic leukemia. *Leukemia* 1999; **13**: 1221–1226.
11 Ross AA, Cooper BW, Lazarus HM, Mackay W, Moss TJ, Ciobanu N, Tallman MS, Kennedy MJ, Davidson NE, Sweet D. Detection and viability of tumor cells in peripheral blood stem cell collections from breast cancer patients using immunocytochemical and clonogenic assay techniques (see comments). *Blood* 1993; **82**: 2605–2610.
12 Borgen E, Beiske K, Trachsel S, Nesland JM, Kvalheim G, Herstad TK, Schlichting E, Qvist H, Naume B. Immunocytochemical detection of isolated epithelial cells in bone marrow: non-specific staining and contribution by plasma cells directly reactive to alkaline phosphatase. *J Pathol* 1998; **185**: 427–434.
13 Pantel K, Schlimok G, Braun S, Kutter D, Lindemann F, Schaller G, Funke I, Izbicki JR, Riethmuller G. Differential expression of proliferation-associated molecules in individual micrometastatic carcinoma cells. *J Natl Cancer Inst* 1993; **85**: 1419–1424.
14 Graham D, Magee H, Kierce B, Ball R, Dervan P, O'Meara A. Evaluation of Ki-67 reactivity in neuroblastoma using paraffin embedded tissue. *Pathol Res Pract* 1995; **191**: 87–91.

References added in proof

15 Méhes G, Luegmayr A, Hattinger CM, Lörch T, Ambros IM, Gadner H, Ambros PF. Automatic detection and genetic profiling of disseminated tumor cells in neuroblastoma. *Med Ped Oncol* (in press).
16 Méhes G, Lörch T, Ambros PF. Quantitative analysis of disseminated tumor cells in the bone marrow by automated fluorescence image analysis. *Cytometry* (in press).

(Circulation. 1995;92:202-205.)

Articles

Generation of Tumor-Specific T Lymphocytes for the Treatment of Posttransplant Lymphoma

J. Michael DiMaio, MD; Peter Van Trigt, MD; J. William Gaynor, MD; R. Duane Davis, MD; Eamonn Coveney, MD, FRCSI; Bryan M. Clary, MD; H. Kim Lyerly, MD

From the Departments of Surgery (J.M.DiM., P.V.T., J.W.G., R.D.D., E.C., B.M.C., H.K.L.) and Pathology (H.K.L.), Duke University Medical Center, Durham, NC.

Background The incidence of lymphoproliferative disease, including B-cell lymphomas (BCL) in patients who have undergone heart or combined heart-lung transplants, has been reported to be as high as 15%. The majority of these tumors contain Epstein-Barr virus (EBV) DNA and regress when immunosuppressive agents are discontinued. This tumor regression is thought to be secondary to cytotoxic T lymphocytes (CTL) reactive to EBV-infected cells whose function is impaired in patients receiving immunosuppressive agents. We hypothesize that EBV-CTL expanded in the absence of these agents may demonstrate an antitumor effect against an EBV-expressing human BCL in vitro and in vivo.

Methods and Results An EBV-expressing BCL from a heart transplant recipient was isolated and expanded in culture. EBV-CTL were generated by stimulation of peripheral blood leukocytes with irradiated autologous tumor cells in low-dose interleukin-2. Autologous BCL, HLA-mismatched BCL, lymphokine-activated killer target cell line (Daudi), and the natural killer target cell line (K562) were used in a standard 4-hour cytotoxicity assay using 51CrO4 after 7, 14, and 28 days of stimulation. There was significant percent specific lysis of autologous BCL targets (78%) at an effector-to-target ratio as low as 20:1 as compared with control cells. EBV-CTL were then adoptively transferred into SCID mice (provided by Duke University Vivarium) that had been engrafted with autologous BCL 7 days before. There was a significant survival advantage to those mice engrafted with EBV-CTL as compared with control cells.

Conclusions The results indicate that ex vivo expansion of EBV-CTL in the absence of immunosuppressive agents results in a population that has significant antitumor activity. This strategy may be useful in the generation of EBV-CTL that might be effective antitumor agents in transplant recipients with EBV-associated lymphomas.

Key Words: lymphocytes • transplantation • cells • heart transplant • lymphoma • immunodeficiency

Introduction

The incidence of lymphoproliferative disease, including BCLs in patients who have undergone heart or combined heart-lung transplants, has been reported to be as high as 15%. The mortality associated with these tumors that appear more than 1 year posttransplant is approximately 70%. The majority of these BCLs contain EBV DNA as demonstrated by DNA hybridization studies, polymerase chain reaction, and immunohistochemistry.1 2 3

As many as 89% of these tumors regress in thoracic organ transplant patients when immunosuppression is discontinued if the tumor appeared within the first year of transplantation.4 5 6 This phenomenon is thought to be the result of the repopulation of EBV-CTL, which are suppressed by cytotoxic agents such as cyclosporine. Therefore, it is hypothesized that autologous EBV-CTL expanded in the absence of these immunosuppressive agents may demonstrate an antitumor effect against an autologous EBV-expressing human BCL in vitro and in vivo.

Methods

Isolation of Posttransplant Lymphoma and Human Cell Lines

After informed consent was obtained a tumor was obtained from a patient who had developed a BCL 7 years after an orthotopic heart transplant for ischemic cardiomyopathy. The tumor was minced and passaged. At surgery, portions of excised tumor were placed in either sterile saline, snap-frozen in liquid nitrogen, or fixed in neutral-buffered formalin. Those portions in saline were mechanically dispersed into single-cell suspensions and layered and placed in culture in 25-cm2 flasks (CoStar) with RPMI 1640 (Sigma Chemical Co)/20% FCS with supplemental antibiotics. BJAB is an ATCC (American Type Culture Collection, Rockville, Md) line isolated from human Burkitt's lymphoma that is EBV negative.

FACS Analysis

FACS was performed by single- or double-staining of isolated cells by direct techniques using phycoerythrin- or fluorescein isothiocyanate–conjugated monoclonal antibodies. Cells were washed with cold PBS containing 0.5% BSA and 0.1% NaN3. The cells were then incubated with directly labeled antibodies for 30 minutes at 4°C. The cells were washed and analyzed in an EPICS C flow cytometer (Coulter) at 488 nm for percent positivity on a log fluorescent scale. Background control tubes were incubated with directly labeled class-matched mouse Igs. Monoclonal antibodies CD4 (OKT4), CD8 (OKT8), and CD19 (OKB-PanB) from Ortho Diagnostics and CD3 (Leu-4), CD19 (Leu-12), CD20 (Leu-16), CD22 (Leu-14), CD23 (Leu-20), and CD56 (Leu-19) from Becton-Dickinson were used for single and dual color-flow cytometry.

SCID Mice

SCID mice were obtained from a hysterectomy-rederived central inbred colony of defined flora-gnotobiotic stock maintained at Duke University. After transfer to a biosafety level 3 isolation facility, mice were maintained in filter-capped Micro-Isolator cages (Lab Products Inc). Cages were housed within a HEPA-filtered Blickman isolator system (Blickman), and mice were fed sterilized rodent chow. Before all manipulations, Micro-Isolator cages were transferred to a laminar flow Bioguard hood (The Baker Co), and animals were handled aseptically by investigators wearing sterile gloves, masks, and gowns. Blood samples were obtained from all mice

before their induction into experiments by retroorbital sinus bleeding. Serum from mice was screened for murine Ig by ELISA and total murine Ig levels were quantified using goat antimouse Ig. Mice with Ig levels greater than 0.01 mg/mL, indicative of leakiness of the SCID defect, were excluded from study.

Histopathology

The primary human tumor and SCID mice tumors were processed simultaneously. Formalin-fixed specimens were dehydrated and embedded in paraffin, and 5-μm sections were cut and stained with hematoxylin and eosin for morphological evaluation.

Immunohistochemistry

Frozen sections (5 μm) prepared in the usual fashion were stained by an avidin-biotin procedure with a panel of monoclonal antibodies including CD20 (L26, B cell antigen; Dako), CD3 (pan-T cell antigen; Becton-Dickinson), and CD45 RO (UCHL-1, pan leukocyte antigen; Dako).

Frozen sections were also stained with antibodies to EBNA 2 (EBV-encoded nuclear antigen 2) and LMP-1 (EBV-encoded latent membrane protein) from Dako Corp.

Both frozen and paraffin sections were stained with polyclonal rabbit antihuman to kappa and lambda Ig light chain (Calbiochem-Behring Corp) for determination of clonality.

In Situ Hybridization

A biotinylated probe for EBV-DNA (Epstein-Barr virus Bioprobe-labeled probe; Enzo Diagnostics) was used for the detection of EBV genomes in formalin-fixed sections.

Generation of Anti–EBV CTL

Peripheral blood from the patient was diluted 1:3 with PBS and layered over a Ficoll-Hypaque gradient. The mononuclear cell layer was then washed twice and cocultivated with gamma-irradiated BCL in AIM-V media with 5% heat-inactivated autologous plasma for 7 days at a concentration of 1x106 cell/mL with a responder-to-stimulator ratio of 5:1. Repeated stimulations of EBV-CTL were performed at days 7 and 21 with irradiated BCL and a similar responder-to-stimulator ratio. After the second stimulation, recombinant interleukin-2 (rIL-2); 10 IU/mL, Chiron) was added, and the cells were counted and expanded every 3 days with the addition of fresh rIL-2.

Cytotoxicity Assay

Target cells were incubated with 51CrO4 washed, resuspended at 5x104 cells/mL, and combined in triplicate wells of 98-well round-bottom plates with effector cells for E-T (effector to target) ratios of varying numbers. Final volumes of each well were adjusted to 0.2 mL with AIM-V media. Wells containing only culture media and target cells or 5% triton and target cells served as spontaneous and maximum 51Cr release controls, respectively. The plates were incubated at 37°C in 5% CO2 for 4 hours; then 0.10 mL of medium from each well was removed for counting in a Packard Prias gamma spectrometer. Percent specific lysis was calculated by standard methods.

Tumor Cell Engraftment and Development

A reliable and reproducible model of human B-cell tumors (SCID-BCL) in SCID mice has been developed in this laboratory. After engraftment with PBL (peripheral blood leukocytes), engraftment with PBL followed by inoculation with EBV, and engraftment of LCL (lymphoblastoid cell line) results in the development of B cell tumors. To test the effect of adoptive transfer of EBV-CTL on SCID/BCL development 25x106 EBV-CTL were inoculated into the peritoneal cavity of SCID mice 7 days after IP inoculation of 5x106 tumor cells or Dulbecco's PBS (Gibco). Mice were monitored twice weekly, weight and examination for tumor development. Mice were anesthetized with halothane (Fluothane; Ayerst), killed by cardiac puncture, and autopsied. At autopsy, thoracic and abdominal cavities were examined, and tumors were sectioned and cryopreserved in liquid nitrogen or fixed in 10% neutral-buffered formalin. All procedures were approved and conducted in accordance with institutional guidelines.

Results

Pathology

The patient's primary tumor and those that developed in the SCID mice were polyclonal B-cell type as shown in Fig 1. The presence of EBV was confirmed in the primary patient's tumor and the SCID mice by in situ hybridization as seen in Fig 2. FACS analysis revealed significant staining of the tumor cells with B-cell markers CD 19 (95%) and 20 (84%) as well as the EBV receptor CD21 (92%). The EBV viral products EBNA 2 and LMP were noted by immunohistochemistry.

Figure 1. Representative hematoxylin and eosin stain of EBV expressing posttransplant B-cell lymphoma. (magnification x100; inset, x10.)

Figure 2. Representative EBV in situ hybridization stain of EBV-expressing posttransplant B-cell lymphoma from patient or engrafted into SCID mice. (magnification x100.)

FACS Analysis

As shown in the Table, the EBV-CTL generated progressed to 97% CD3+ (pan-T cell) and 88% CD8+ (cytotoxic T cell) after 28 days of stimulation. The majority of CD8+ cells were positive for S6F1 (cytotoxic T cell). The population of B cells or natural killer (NK) target cells diminished with time, to near zero.

Table 1. FACS Analysis of Cells in Culture

Cytotoxicity Assay

Effective cytolysis of the autologous targets was demonstrated by EBV-CTL 7, 14, and 21 days after stimulation as seen in Fig 3. No cytolysis of HLA-mismatched EBV-expressing cell lines was seen. Minimal cytolysis of the NK target K562 was seen on day 7, which diminished by day 14. There was no activity against LAK (lymphokine activated killer) cell target Daudi (data not shown).

Figure 3. Cytotoxicity assay of anti-EBV CTL 7 (A), 14 (B), and 21 (C) days after stimulation with autologous lymphoma cells. Percent specific lysis at various effector-target ratios for EBV-specific CD8+CTL against autologous posttransplant lymphoma cells (autologous), EBV-positive HLA-unmatched cells (HLA mismatched), and a natural killer target cell, K562 (NK).

Adoptive Transfer of EBV-CTL

Results of SCID-BCL and BJAB-BL engraftment and survival as well as the inoculation of EBV-CTL are shown in Fig 4. Engraftment of posttransplant B-cell lymphoma and Burkitt's lymphoma led to the characteristic tumor development and death of the animals in 50 days. Animals inoculated with EBV-CTL 7 days after engraftment with the EBV-negative cell line BJAB (Burkitt's lymphoma) showed no significant difference in survival from the animals engrafted with tumor and then given PBS (P=NS via log rank test). In contrast, animals given autologous EBV-CTL 7 days after engraftment of EBV-expressing BCL had no deaths (P<.05 via log rank test).

Figure 4. A, Kaplan-Meier survival curves of SCID mice engrafted with EBV-expressing posttransplant B-cell lymphoma (Post Tx-BCL) and PBS compared with EBV-expressing posttransplant B-cell lymphoma followed by autologous EBV-specific cytotoxic T lymphocytes (Post-Tx BCL+CTL). There was a significant difference (P<.05) as determined by the log rank test. **B,** Kaplan-Meier survival curves of SCID mice engrafted with EBV-negative B-cell Burkitt's lymphoma (BJAB-BL) and PBS compared with EBV-negative Burkitt's B-cell lymphoma followed by EBV-specific cytotoxic T lymphocytes (-BJAB-BL+CTL). There was no significance difference (P=NS) as determined by the log rank test.

Discussion

Cell-mediated immune responses to EBV infection are considered to be more crucial to the outcome of infection than the humoral responses. A lymphocytosis is composed primarily of CD3+/CD8+ T lymphocytes and is usually seen in acute EBV infection. This early response appears to be a polyclonal T cell activation. Two to 8 weeks after active EBV infection, a more EBV-specific T-cell response can be seen by in vitro proliferation to viral antigen and EBV-specific HLA-restricted lysis of EBV-infected B cells.7 8 9 EBV-CTLs have been cloned from the blood of EBV seropositive donors and inhibit cytotoxicity that is highly specific for EBV-infected cells and are HLA restricted.10 11

Wherever productively infected cells are cleared by the immune system, latently infected B cells persist for the life of the host. In fact, B cells infected with EBV become immortalized B-cell lines and provide a model system of EBV latency.12 13

Evidence suggests that cellular immune response may be effective in controlling EBV-associated LPDs and BCLs in patients who have undergone transplantation.14 15 The term LPD applies to the development of continuously proliferating B lymphocytes, presumably stimulated by EBV infection. This is believed to be related to the failure of the immune system, especially the T-cell population, which is suppressed by drugs such as cyclosporine, to respond normally to EBV-infected B lymphocytes.16 17 The fact that the risk of LPD and the mortality from it increases

with the duration of immunosuppression adds validity to this theory. In approximately 89% of patients in whom BCL developed within 1 year of transplantation, there was complete regression of the lesions after reduction of immunosuppressive therapy alone.18 19 Thus, the decrease in number or function of EBV-CTL may allow for unchecked proliferation of EBV-driven LPD.

One report on EBV-associated LPD after allogeneic bone marrow transplantation documented successful eradication of disease after infusions of donor-derived pooled leukocytes. Because of the known high-frequency of EBV-specific CTL precursors in the blood of seropositive normal donors, it is reasonable to suggest that donor-derived EBV-reactive T cells had a critical role in the response noted. More specific therapy with just EBV-CTL may provide a tailored approach with less systemic side effects. Continued study of the mechanisms underlying the cause of EBV-driven LPD and the cellular immune response, including the EBV-specific CTL response to it, may provide novel treatment strategies against BCLs in the organ-transplant recipient.

0022-1554/91/$3.30
The Journal of Histochemistry and Cytochemistry

Vol. 39, No. 11, pp. 1495–1506, 1991
Printed in U.S.A.

Original Article

Three-dimensional Electron Microscopy of Ribosomal Chromatin in Two Higher Plants: A Cytochemical, Immunocytochemical, and In Situ Hybridization Approach[1]

PATRICK M. MOTTE,[2] ROLAND LOPPES, MONIQUE MENAGER, and ROGER DELTOUR

Laboratoire de Morphologie Végétale (PMM,RD) et de Génétique Moléculaire (RL), Département de Botanique, Université de Liège, B4000 Liège, Belgium, and Laboratoire d'Histologie, Embryologie et Cytogénétique, Faculté de Médecine, 51100 Reims, France (MM).

Received for publication January 15, 1991 and in revised form May 20, 1991; accepted May 31, 1991 (1A2211).

We report the 3-D arrangement of DNA within the nucleolar subcomponents from two evolutionary distant higher plants, *Zea mays* and *Sinapis alba*. These species are particularly convenient to study the spatial organization of plant intranucleolar DNA, since their nucleoli have been previously reconstructed in 3-D from serial ultra-thin sections. We used the osmium ammine-B complex (a specific DNA stain) on thick sections of Lowicryl-embedded root fragments. Immunocytochemical techniques using anti-DNA antibodies and rDNA/rDNA in situ hybridization were also applied on ultra-thin sections. We showed on tilted images that the OA-B stains DNA throughout the whole thickness of the section. In addition, very low quantities of cytoplasmic DNA were stained by this complex, which is now the best DNA stain used in electron microscopy. Within the nucleoli the DNA was localized in the fibrillar centers, where large clumps of dense chromatin were also visible. In the two plant species intranucleolar chromatin forms a complex network with strands partially linked to chromosomal nucleolar-organizing regions identified by in situ hybridization. This study describes for the first time the spatial arrangement of the intranucleolar chromatin in nucleoli of higher plants using high-resolution techniques. (*J Histochem Cytochem 39:1495–1506, 1991*)

KEY WORDS: Nucleolus; rDNA; Nucleolus-associated chromatin; Root cells; Anti-DNA antibody; Osmium ammine; *Zea mays*; *Sinapis alba*.

Introduction

The chromatin organization of the interphase nucleus has been investigated for many years. From recent data, we can argue that interphase chromosomes occur in well-defined nuclear domains (8,21,29,30,36,37). Concerning the nucleolar chromatin, it is well known that each metaphasic nucleolus organizer region (NOR), which contains the genes coding for the precursors of ribosomal RNA (rDNA), is a well-defined part of an NOR-bearing chromosome. The number of NOR-bearing chromosomes varies according to the species. At the end of telophase each NOR, or part of it, is responsible for the formation of one nucleolus (9,11,17,31). During interphase the nucleoli may fuse together. However, the exact localization of the nucleolar chromatin, i.e., of the rDNA molecule, within the active nucleolus is still unknown and is the subject of controversy (see Discussion). Its three-dimensional distribution is still totally unknown. By electron microscopy, five subcomponents can be distinguished in a transcriptionally active nucleolus: the fibrillar centers (FCs), the dense fibrillar component (DFC) which surrounds the FCs, the granular component (GC), the highly contrasted nucleolus-associated chromatin (NAC) observed at the periphery of the nucleolus, and small, less electron-opaque spaces, referred to as nucleolar vacuoles.

The unambiguous localization of rDNA in these subcomponents could be essential for the understanding of the functional organization of the nucleolus. In the present study we have used DNA-specific osmium ammine staining on thick sections, immunocytochemical technique, and in situ hybridization to localize rDNA and to study its spatial distribution in an active plant nucleolus at the electron microscopic level. Compared with animal material, the plant cell nucleolus exhibits specific advantages: (a) The NAC, restricted to heterochromatic knobs located at the nucleolar periphery, are parts of the interphasic NORs (32,36,37; and this report). On the contrary, in animal nucleoli, a peripheral ring of NAC of an unknown nature is always observed. The relationships between this peripheral chromatin and the intranucleolar rDNA are not well defined (43); (b) the DFC is large and constitutes the main structure of the plant active nucleolus; and (c) the active nucleoli of the two plant species here studied have been previously three-dimensionally reconstructed from serial ultra-thin sections (10,32).

[1] Supported by grants from the FRFC (2.405.87 and 2.4521.89) and from "Action de Recherche Concertée" (88/93.129).

[2] Correspondence and present address: Dr. Patrick M. Motte, Max-Planck-Institut für Züchtungsforschung, 10 Carl-von-Linné Weg, D-5000 Köln 30, Germany.

The localization and spatial arrangement of ribosomal chromatin is discussed and compared with the recent data on rDNA distribution in both plant and animal nucleoli.

Materials and Methods

Germination Procedure

Batches of 30 seeds of *Zea mays* and *Sinapis alba* were germinated in petri dishes on cotton wool and filter saturated with distilled water. They were incubated in darkness in an Ehret-controlled temperature chamber at 16°C and 9°C, respectively. Germination began when the seeds were placed in contact with water. The maximum percentage of germinated seeds was always over 90%, and the rates of germination were very similar for both species. One hundred twenty hours after germination embryonic roots were about 3 cm in length.

Tissue Preparation

The distal millimeter of roots was excised from quiescent embryos and, 120 hr after sowing, rapidly immersed in a solution of 4% formaldehyde (freshly prepared from paraformaldehyde) in 0.1 M Sorensen buffer (pH 7.0) and maintained for 2 hr at room temperature. The root caps were excised and discarded. The root fragments were washed three times in 0.1 M Sorensen buffer at 4°C. The samples were then embedded in Lowicryl K4M at low temperature according to Carlemalm et al. (6) with longer infiltration periods. Semi-thin and ultra-thin sections were cut with a diamond knife in the cortex 1 mm from the root tips with a Sorval Porter Blum MT2 ultramicrotome. After the reactions described below, the sections were observed with a Siemens Elmiskop 101 or a Zeiss electron microscope EM109 at 80 kV.

Osmium Ammine-B (OA-B) Staining

OA-B was synthesized according to Olins et al. (33). Semi-thin sections about 0.5 µm thick realized in maize and *Sinapis alba* root fragments were mounted on 300-mesh gold grids without formvar support. Before the OA-B staining the sections were treated with 1 mg/ml pre-digested pronase (Boehringer; Mannheim, FRG) for 1 hr at 37°C in Tris-HCl 10 mM (pH 7.2). For the staining, the grids were first floated, sections facing the solution, on the surface of a 5 N HCl solution for 25 min at room temperature. The grids were then thoroughly washed with distilled water and floated on some drops of water until osmium ammine-B solution was ready. A 0.2% aqueous solution of OA-B was bubbled with SO_2 for 20 min. The staining of DNA was performed for 60 min at 37°C in a well-covered container, sections floating on the solution. The grids were thoroughly jet-washed with distilled water. We performed successively two ultra-thin and one semi-thin serial sections. The two ultra-thin sections were stained with uranyl and lead (Ur-Pb), while the thick section was stained with OA-B.

Some thick sections were observed with a Jeol 200CX at 200 kV. Sections were tilted with an eucentric goniometer stage from −18 to +18° by 6° steps. Stereo pairs of tilted images were mounted to be observed with a pocket stereoviewer according to Ploton et al. (35).

Electron Microscopic Immunocytochemistry

Yellow ultra-thin sections of embedded *Zea mays* fragments were mounted on formvar-coated gold grids. For labeling the grids were processed at room temperature as described below. The sections were incubated on 20 µl of PBS, pH 7.5, containing 0.5% BSA, 0.1% Tween 20 (PBST), and normal goat serum diluted 1:20, for 30 min. Then the grids were floated on 10 µl of PBS containing IgM mouse monoclonal DNA antibodies (30 µg/ml; Boehringer) and 1:50 normal goat serum, for 3 hr. The grids were washed with PBST twice for 10 min, then were incubated on 20 µl of PBST (pH 8.2) containing 1:75 goat anti-mouse IgM coupled to 5-nm gold particles

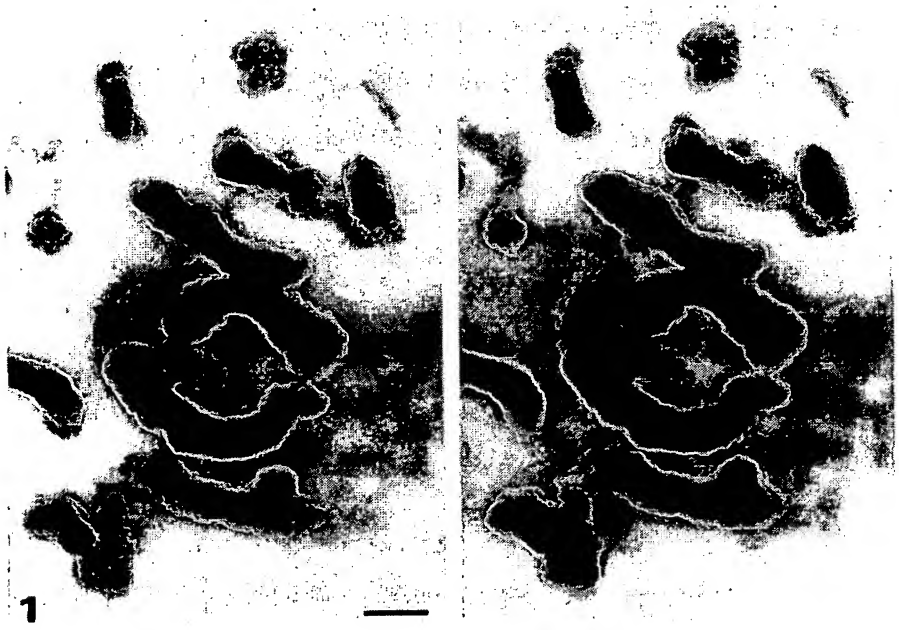

Figure 1. Stereo pair of *Zea mays* metaphase chromosomes stained with OA-B complex, observed at 200 kV. One-µm thick section. Long chromosome segments located at different level in the section are stained all along their length without interruptions. This demonstrates that the OA-B complex penetrates through the entire Lowicryl section. Note that when a chromosome is longitudinally sectioned the portion within the section is less thick and thus is less stained. Original magnification × 6800. Bar = 1 µm.

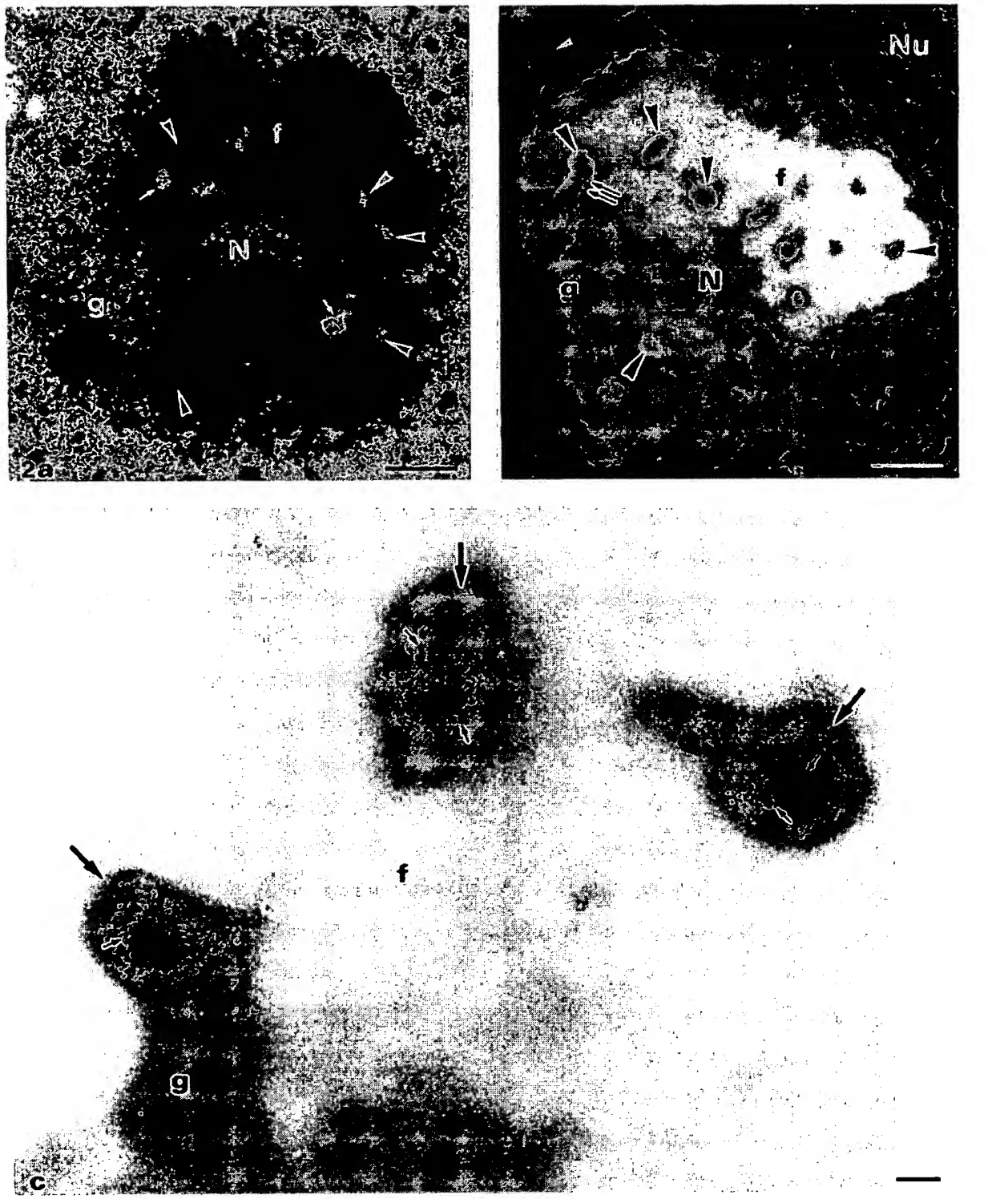

Figure 2. (a) Electron micrograph of a Lowicryl K4M-embedded nucleolus (N) of *Zea mays*, a monocotyledon. The subcomponents are visible and well discriminated: the DFC (f) is the main component surrounding a few FCs (arrowheads) often associated with small vacuoles or interstices (small arrows). The whole fibrillar component (DFC and FCs) which forms the nucleolonema is enclosed within the granular component (g). Uranyl and lead staining. (b) Semi-thin section of a nuclear portion of *Zea mays* stained with osmium ammine-B complex. The DNA-containing structures are well contrasted in the nucleoplasm (Nu). At low magnification, the nucleolar subcomponents are still easily visible owing to their remnant electron opacity after the pronase digestion. The DFC (f) appears like homogeneous bleached large zones and the GC (g) like interspersed clear gray and bleached zones. The FCs (arrowheads) appear like small contrasted areas embedded in the DFC and contain DNA stained by the OA-B complex. In some cases the granular component is directly in contact with a fibrillar center (double arrows). The cytoplasmic DNA is also visible (white arrowhead). (c) High magnification of the three upper left FCs (arrows) of b. Clumps of chromatin fibers (small arrows) are well visible inside small areas probably corresponding to FCs. DNA fibers are not observed within the surrounding DFC (f). g, granular component. Original magnifications: a,b × 6000; c × 20,000. Bars: a,b = 1 μm; c = 0.1 μm.

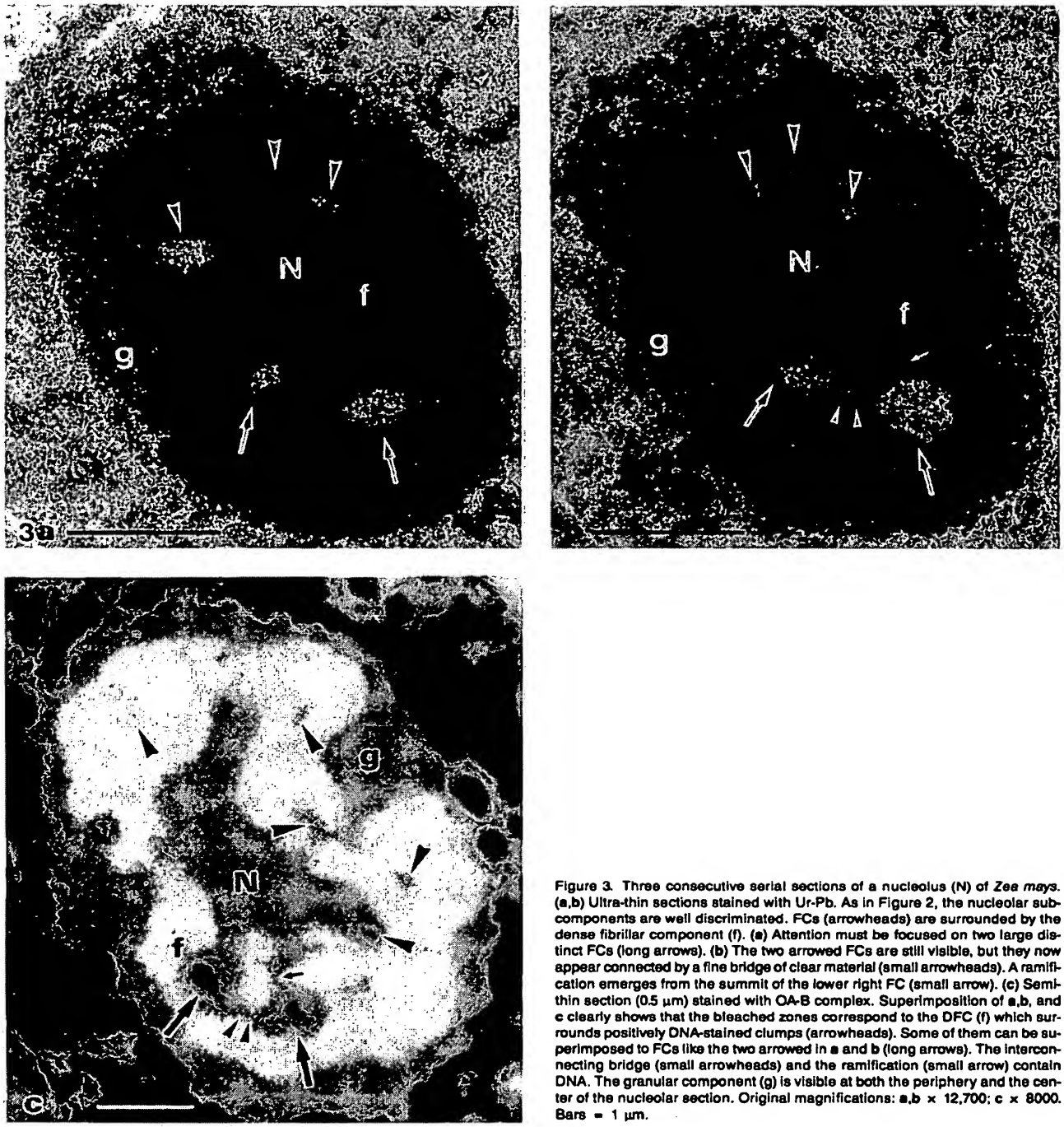

Figure 3. Three consecutive serial sections of a nucleolus (N) of *Zea mays*. (a,b) Ultra-thin sections stained with Ur-Pb. As in Figure 2, the nucleolar subcomponents are well discriminated. FCs (arrowheads) are surrounded by the dense fibrillar component (f). (a) Attention must be focused on two large distinct FCs (long arrows). (b) The two arrowed FCs are still visible, but they now appear connected by a fine bridge of clear material (small arrowheads). A ramification emerges from the summit of the lower right FC (small arrow). (c) Semithin section (0.5 μm) stained with OA-B complex. Superimposition of a,b, and c clearly shows that the bleached zones correspond to the DFC (f) which surrounds positively DNA-stained clumps (arrowheads). Some of them can be superimposed to FCs like the two arrowed in a and b (long arrows). The interconnecting bridge (small arrowheads) and the ramification (small arrow) contain DNA. The granular component (g) is visible at both the periphery and the center of the nucleolar section. Original magnifications: a,b × 12,700; c × 8000. Bars = 1 μm.

(Janssen Life Sciences; Beerse, Belgium) for 60 min. The grids were rinsed three times for 10 min in PBST and three times in distilled water. The sections were stained with uranyl acetate. Controls were performed by incubating sections with either distilled water, PBS, or normal mouse serum in place of the anti-DNA antibody. Ultra-thin sections labeled with the anti-DNA antibody were also stained by the OA-B as described above, without pronase digestion.

In Situ Hybridization Procedure

Preparation of the Biotinylated Probe. Plasmid pMrl (48) contains parts of the 25S and 18S rRNA coding regions and one complete spacer region of a maize rRNA transcription unit. The 0.75 KB Sma I fragment of the 25S rRNA coding sequence was subcloned into pUC9. The presence in the insert of Bgl II and Bam HI sites was verified. One microgram of the plas-

mid (pULG-1) was labeled with biotin-11-dUTP by nick translation using the BluGENE kit from Bethesda Research Laboratories (Gaithersburg, MD). The probe was purified by gel filtration on Sephadex G-50, precipitated by ethanol, then dissolved in 50 µl sterile water and stored at −20°C. Spots of 6 pg (in 3 µl) of the probe were easily detected on nitrocellulose filters using streptavidin–alkaline phosphatase conjugate, then nitroblue tetrazolium and 5-bromo-4-chloro-3-indolylphosphate according to the recommendations of the supplier.

In Situ Hybridization (rDNA–rDNA). Yellow sections of *Zea mays* samples, collected on formvar-coated gold grids, were first submitted to enzymatic digestions performed at 37°C in a moist chamber. The sections were digested for 1 hr by 1 mg/ml pre-digested pronase in 10 mM Tris-HCl (pH 7.2), then treated for 1 hr by pre-boiled RNAse (1 mg/ml in 10 mM Tris-HCl, pH 7.2). The grids were then subjected to three 10-min rinses in distilled water and air-dried. Cellular DNA was denatured for 10 min at 80°C in 75% (v/v) deionized formamide in 2 × SSC (1 × SSC = 0.15 NaCl, 0.015 M sodium citrate, pH 7.0). The sections were then immediately dipped into ice-cold 0.1 × SSC, dehydrated in an ethanol series of 50%, 75%, and absolute ethanol, and air-dried for a few minutes. The probe diluted in the hybridization buffer (50% deionized formamide/10% dextran sulfate/1 × Denhardt's solution/1 mM EDTA/600 mM NaCl/500 µg.ml^{-1} herring sperm DNA/25 mM Tris-HCl, pH 7.2) was denatured for 4 min at 100°C. Hybridization buffer contained biotinylated probe at 0.8–1.0 µg/ml. The grids were floated overnight at 40°C in a moist chamber on 5 µl of the denatured hybridization solution. Grids were then floated three times for 10 min on drops of PBS, incubated successively in mouse anti-biotin antibody (Dako; Santa Barbara, CA) and goat anti-mouse IgG conjugated to gold particles 3–5 nm in diameter (Janssen), and finally stained with uranyl acetate before examination. Controls were performed by incubating sections on either hybridization buffer or hybridization buffer containing the biotinylated pUC9 plasmid.

Results

One hundred twenty hours after the onset of germination, the fully functional nucleolus was capable of both synthesizing and processing pre-rRNAs (50). It was composed of well-segregated granular and fibrillar components.

Osmium Ammine-B Staining

The osmium ammine complex is known to be a specific stain for DNA in electron microscopy (12,13). To increase the contrast of the chromatin fibers and to study three-dimensionally the intranucleolar

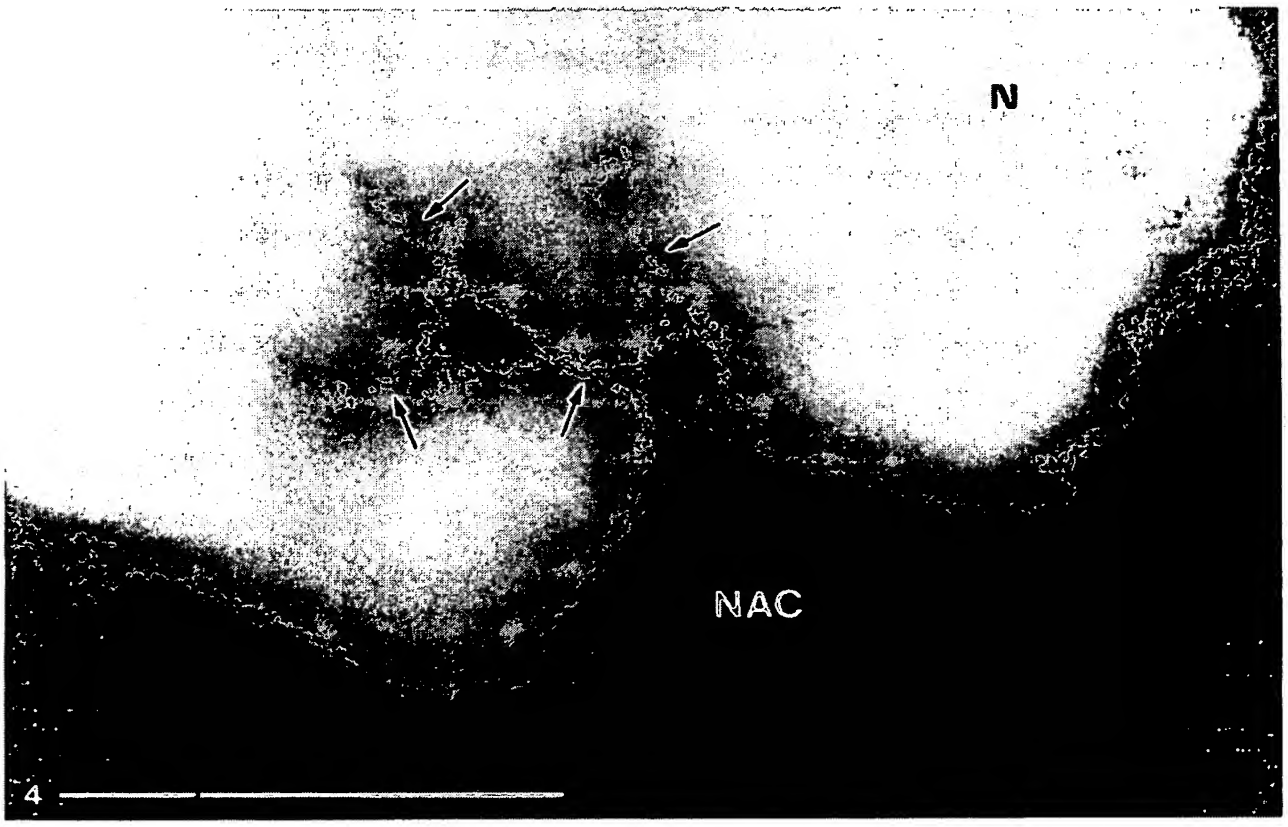

Figure 4. Semi-thin section of a maize nucleolus (N) stained with OA-B complex. One peripheral knob of the nucleolus-associated chromatin (NAC) is visible, from which a continuous and multibranched DNA-containing structure intrudes into the nucleolus. The ramifications are shown by arrows. Original magnification × 22,000. Bar = 1 µm.

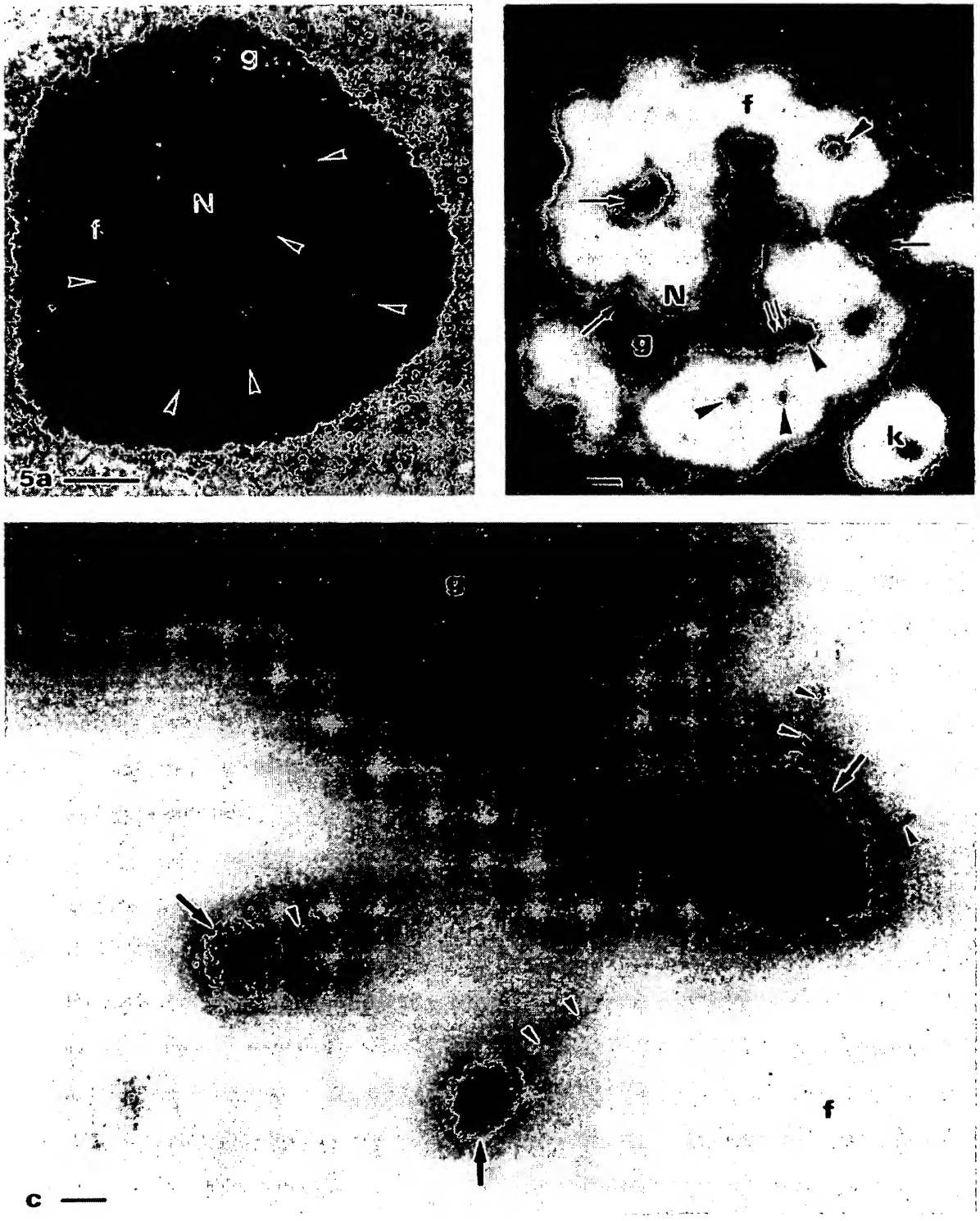
g
N
f
5a
f
N
g
k
f
c

DNA, the OA-B reaction was applied on semi-thin sections of Lowicryl K4M-embedded root fragments. In this polar embedding resin, the OA-B complex stained the DNA-containing structures throughout all the semi-thin section thickness, as seen very well on the tilts of the metaphasic chromosomes (Figure 1). It must be noted that in Lowicryl K4M sections the OA reaction is specific for the nucleic acids (12). However, the pre-treatment with hydrochloric acid removes all the ribonucleic acids from the section. Different times of HCl hydrolysis (from 10–35 min) were realized without modification of the specificity and quality of the staining (data not shown). When a DNAse digestion was performed, the contrast of DNA-containing structures disappeared (unpublished results). We performed a pronase digestion before OA-B staining to strongly decrease the electron opacity of the nucleolar section under the EM, which was mainly due to proteins. In our material and working conditions very good staining of chromatin fibers was obtained in *Zea mays* (a monocotyledon) as well as in *Sinapis alba* (a dicotyledon) (Figures 2–6). After the OA staining on thick sections the DNA was heavily stained in both the cytoplasmic organelles (mitochondria and plastids) and the nucleus (Figures 2 and 5). In the nucleoplasm, irregular clumps of chromatin, sometimes in contact with the nuclear envelope, were densely stained. From them, fine non-nucleosomal DNA filaments about 3 nm thick emerged and irradiated within interchromatin zones (data not shown). A large roundish space corresponding to the nucleolar body showed bleached areas surrounding some entities of higher electron opacity containing contrasted DNA filaments. The bleached areas correspond to the dense fibrillar component, which is known to contain a large amount of proteins (25,28). The small areas surrounded by the DFC correspond to the FCs. The granular component appeared like interspersed clear gray and bleached zones. To unambiguously identify the nucleolar subcomponents, we performed superimposition of successive ultra-thin sections stained with Ur-Pb and a thick section stained with the OA-B complex. Comparison of Figures 3a, 3b, and 3c clearly showed that the entities within the DFC were FCs containing chromatin fibers. Moreover, the DNA localization was sometimes restricted to particular regions of the FCs. The DFC and the GC did not contain any detectable DNA. At higher magnification on ultra-thin sections stained with OA-B, 10–13-nm thick granules considered as nucleosomes were seen in the FCs (Motte et al., manuscript in preparation). On some sections we could see very well the continuity and the ramifications of the intranucleolar chromatin which is located in a complex network (Figures 4–6). The internal NAC appeared to be ramified as soon as it intruded within the nucleolus (Figure 4). The ramifications were often visible at the level of large masses of dense chromatin probably corresponding to the core of the heterogeneous FCs (Figure 6). In some rare sections, loops of internal NAC were observed (data not shown).

Immunocytochemical Localization of DNA

We localized the DNA by means of a mouse monoclonal antibody directed against single- and double-stranded DNA. Immunolabeling was performed on ultra-thin Lowicryl sections. After the immunoreactions gold particles were essentially observed over the dense chromatin in the nucleus (Figure 7) and over the clumps of dense NAC located at the nucleolar periphery (not shown). Large nucleoplasmic areas were devoid of labeling. Over the nucleolus, gold particles were present over electron-clear areas corresponding to FCs. On some sections the labeling was observed at the border of the FCs (Figure 7a). To compare the respective efficiency of the OA-B complex and the anti-DNA antibody, we stained ultra-thin Lowicryl sections by both methods. We observed that the gold particles were strictly located over structures stained with the osmium ammine-B complex, but the density of gold particles over the dense chromatin was weak (Figure 7b). This is due to the reaction of the anti-DNA antibody with only the DNA molecule at the surface level of the section, whereas the OA-B stains DNA included in the entire section thickness. Thus, the use of the anti-DNA antibody is insufficient to reveal the continuity of the intranucleolar chromatin.

In Situ Hybridization

We performed in situ hybridization on ultra-thin Lowicryl sections of quiescent maize embryos because the quiescent state offers certain advantages: the NAC appears like two knobs adjacent to the periphery of the nucleolus, is very compact, and permits high signal/background labeling. Indeed, after the in situ hybridization we saw very well the gold particles concentrated in the region corresponding to the NAC (Figure 8). Therefore, these knobs correspond to the NORs which, as previously shown, stretch out and run inside the nucleolus during early germination.

Discussion

Localization of DNA in the Interphase Nucleolus

Previous ultrastructural and cytochemical studies have suggested the presence of DNA in the fibrillar component of plant and animal nucleoli (1,17,28). More recently, by means of the OA reaction

Figure 5. (a) Electron micrograph of a nucleolus (N) of *Sinapis alba*, a dicotyledon. The dense fibrillar component (f) appears as large electron-opaque areas surrounding many small FCs (arrowheads). The granular component (g), which is more compact than in maize, envelopes the entire fibrillar component. (b) Semi-thin section of a nucleolus (N) of *Sinapis alba* stained with OA-B complex. As in maize, one can clearly recognize the strongly bleached DFC (f) surrounding small FCs (arrowheads) which react positively with OA-B. The granular component (g) appears like a homogeneous clear gray zone. Note that, first, the GC is frequently observed in close contact with FCs (double arrows), and second, nucleolar vacuoles (long thin arrows) are present in both the DFC and GC. They appear as areas slightly more electron opaque than the GC. This is due to the intrinsic opacity of the acrylic resin, which is more abundant in this nucleolar subcomponent. In the DFC the vacuoles are always associated with the DNA internal to FCs. k is probably a karyosome. (c) High magnification of the three bottom right FCs (arrows) of b showing the DNA clumps located in the FCs. The DFC seems to be devoid of DNA. The contact between the GC (g) and the DNA internal to FCs is particularly well visible. Small threads of DNA (small arrowheads) originate from the large clumps. They are probably ramifications or interconnections between chromatin clumps, as more clearly observed in Figure 6. Original magnifications: a × 4700; b × 6000; c × 20,000. Bars: a,b = 1 μm; c = 0.1 μm.

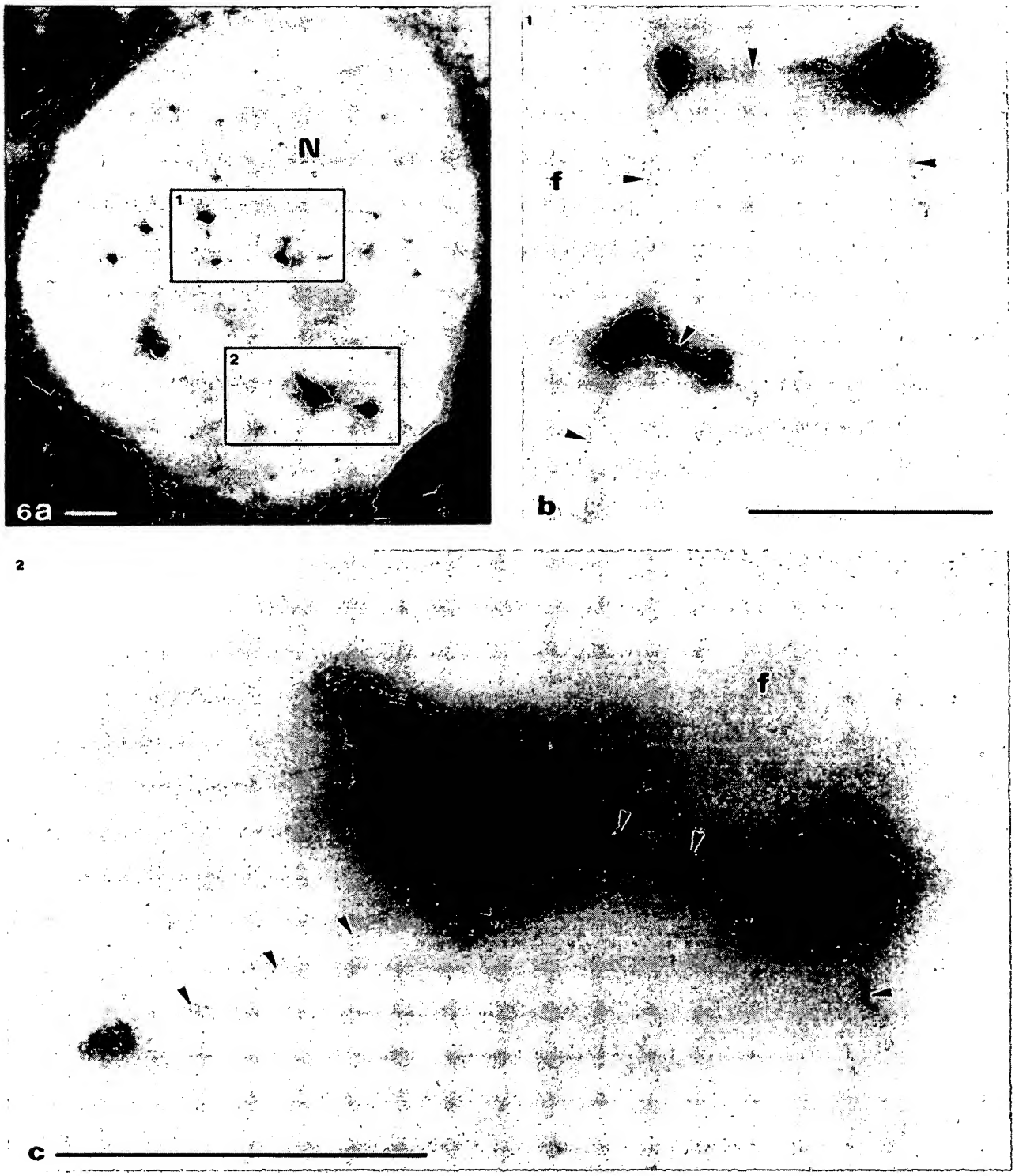

Figure 6. Semi-thin section of nucleolus (N) of *Sinapis alba* stained with OA-B complex. (a) The FCs form a complex network, the interconnections of which are small threads of DNA. (b,c) High magnifications of the two nucleolar portions 1 and 2. The progressive stretching out of the compact DNA (arrows) is clearly apparent (arrowheads). Some ramifications are so thin that they are probably constituted of one or a few rDNA molecules. Original magnifications: a × 4000; b,c × 20,000. Bars = 1 μm.

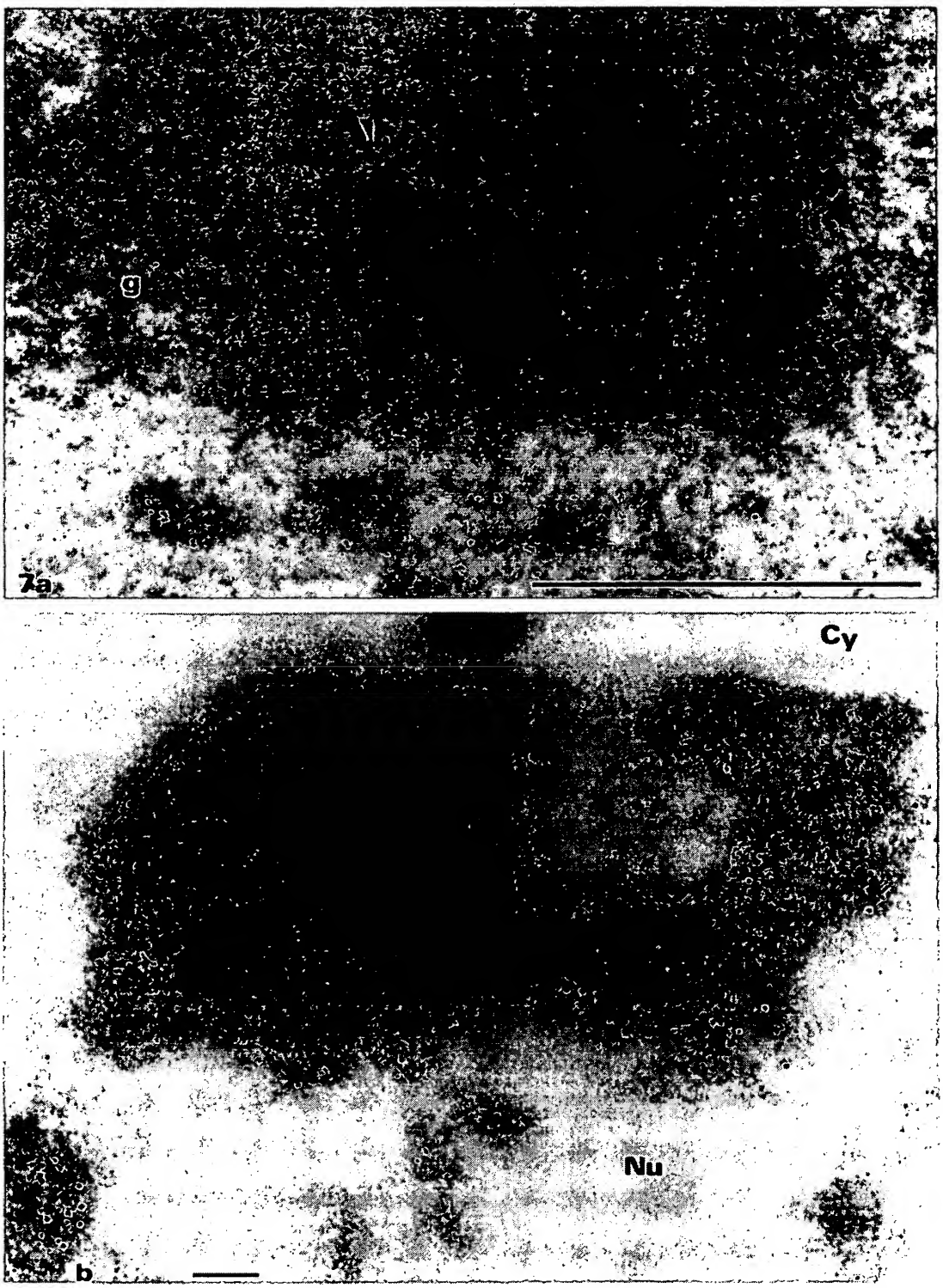

Figure 7. (a) Immunocytochemical localization of DNA on Lowicryl K4M sections of *Zea mays* using a monoclonal anti-DNA antibody. Uranyl staining. (a) View of an FC surrounded by a thick layer of DFC (f). Labeling is present in the FC (arrowheads). The DFC and the granular component (g) are devoid of gold particles. The fibrillar texture of the DFC is well visible on this micrograph. (b) Portion of a nucleus of *Zea mays* labeled with anti-DNA antibody and stained with the OA-B complex. Note that the HCl hydrolysis does not remove the gold particles. If there is a good superimposition of the detection methods, the density of the gold particles is not sufficient to detect all the DNA and to delineate precisely the DNA-containing regions. In contrast, the latter can be strictly mapped by the OA-B complex. Original magnification × 40,000. Bars: a = 1 μm; b = 0.1 μm.

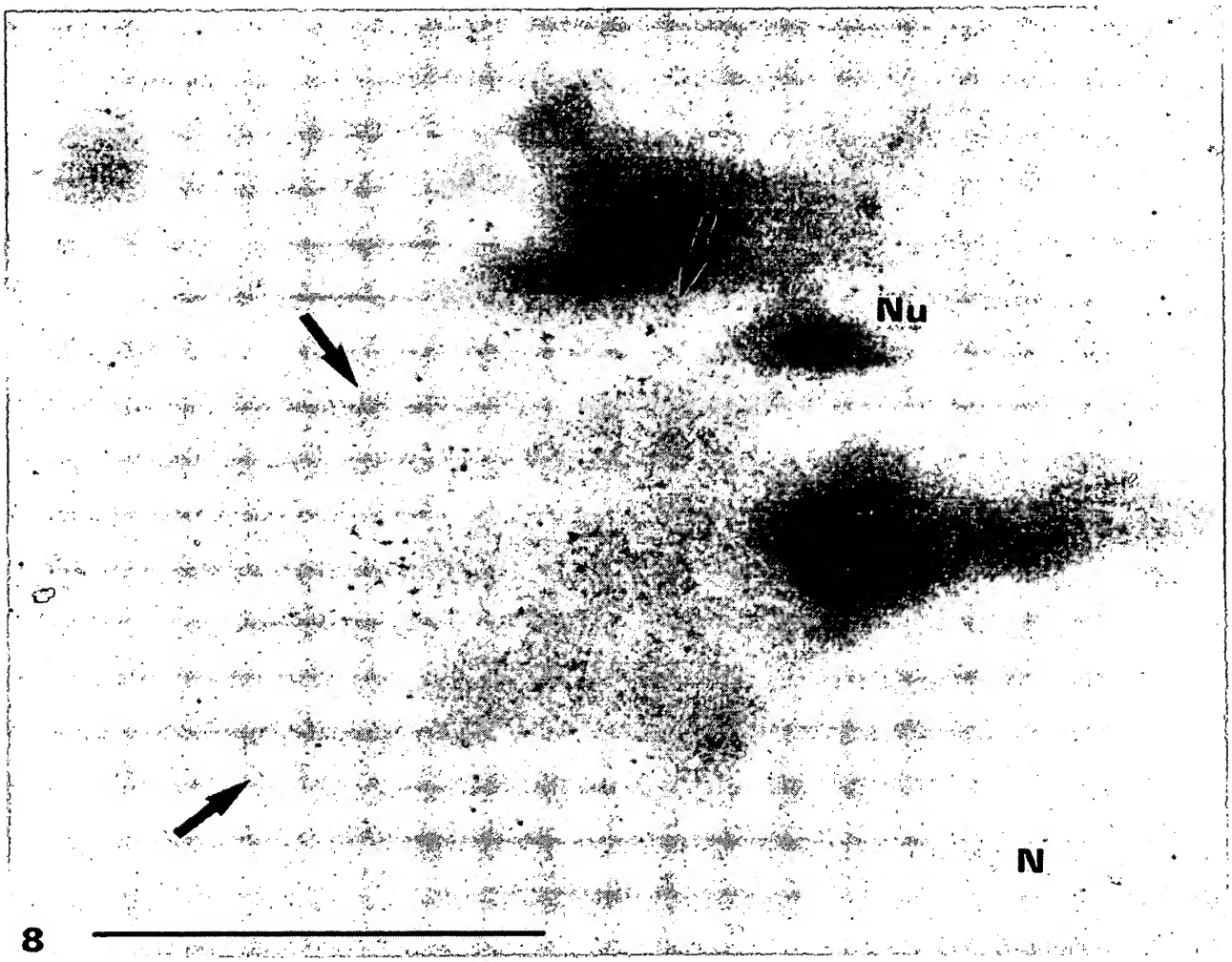

Figure 8. In situ hybridization on protease–RNAse-digested Lowicryl section of a quiescent maize nucleolus (N). The gold particles are restricted to the peripheral knob of the nucleolus-associated chromatin (arrows) in close association with fibers of DNA. The two knobs observed at the periphery of the maize nucleolus correspond to the two nucleolus-organizer regions present in this species. Original magnification × 20,000. Bar = 1 μm.

on animal tissues, Derenzini et al. (13) have established that DNA is present within the FCs and probably in the DFC, and is constituted of extended non-nucleosomal 3-nm thick filaments. However, after the OA reaction the identification of the FCs and tight DFC is not reliable in animal nucleoli. On the basis of qualitative (9,17) and quantitative (15) high-resolution autoradiographic studies, it has generally been admitted that the DFC corresponds to the transcriptionally active part of the interphase NOR. However, autoradiography can be criticized because a displacement of labeled primary rRNA transcripts could rapidly occur and/or the labeling could also result from 5S rRNA synthesized elsewhere in the nucleus and rapidly transferred into the DFC (44). In this connection, some recent biochemical studies have disclosed that the intergene spacer is transcribed in various animal cells (*Xenopus*, *Drosophila*, mammalian species) (3,7,14,20,22,45). The spacer transcripts are highly unstable in vivo and a rapid processing and degradation of them is likely to occur (20,45). Therefore, one can not state with certainty that DFC contains DNA. In addition, some recent immunocytochemical studies have led to challenge of this view. Scheer et al. (41,42) have detected the anti-RNA polymerase I antibodies exclusively in the FCs of various cell lines. A similar nucleolar localization was also found for anti-topoisomerase I and anti-DNA antibodies (38,40,46). Benavente et al. (4,5), using a different approach, support the idea that DFC is a genuine entity not constituted by the superimposition of transcriptional units of rDNA and primary transcripts. The rDNA localization with in situ

hybridization techniques in active animal nucleoli provides controversial results (47,51). Taken together, these results cast doubts on the localization of the primary sites of transcription in the DFC.

In the present study, we detect DNA mainly in the FCs of interphase plant nucleoli. The penetration of the OA complex throughout the section thickness shows any very weak quantity of DNA and thus allows study of the 3-D organization of DNA on thick sections. On semi-thin sections digested by pronase and stained by OA, the nucleolar subcomponents are well discriminated and recognizable by their electron opacity. The nucleolar subcomponents appear like a negative micrograph of an ultra-thin section stained with uranyl and lead. This was confirmed by the superimposition of successive ultra-thin sections and OA-stained thick section. It is beyond doubt that DNA chromatin fibers are located in FCs. A potential problem in the interpretation of our results is the possibility that the processes of the OA staining would specifically destroy the DNA fibers contained in the DFC. Since the OA complex stains very small DNA amounts in the FCs, in the nucleoplasm, and in the cytoplasmic organelles, it follows that if DNA is present in the DFC it should be structurally different and more flimsy than the other DNA fibers. Possibly this could occur following the pronase digestion. However, because we know of no data reporting such observations, this process appears to us highly improbable. Therefore, our results support the studies suggesting that rDNA is localized only in FCs in higher plant (36,37) as well as in animal cells (2,38,40–42,46).

Spatial Organization of the Intranucleolar Chromatin

Early cytological studies on the nucleolus have already described, in light microscopy, an intranucleolar filamentous structure generally called the "nucleolonema" (see 11 for references). These filamentous structures are detected in animal cells after drug treatment (16,18,26,39) or after removal of arginine from the culture medium (19), and in plant cells after treatment of isolated nuclei with a detergent (23,24). The nucleolonema may also appear as a natural structure in the epidermal cells of *Calpodes* in relation to the content of hemolymph ecdysteroid (27). In situ hybridization has shown that in human glioma cells, ribosomal genes form intranucleolar strands 0.2 μm thick (29).

By means of 3-D reconstructions of nucleoli from serial ultra-thin sections in the two species studied here, we have previously shown that the nucleolonema is ramified and appears as an arborescent structure mainly composed of fibrillar material, the axis of which appeared in transverse or oblique sections as homogeneous and heterogeneous FCs (10,32). However, we had no information on the localization of DNA and ribosomal genes in this filamentous structure. In the present study, we have shown a defined 3-D organization of the intranucleolar chromatin which forms a very complex filamentous structure within an active higher plant cell nucleolus. This structure is continuous and ramified. In 3-D reconstructions it was sometimes difficult to follow the continuity of the FCs. Indeed, we see very clearly on thick sections stained with the OA complex that the axis of the nucleolonema (containing DNA) can be so thin at some places (Figures 6 and 7) that it cannot be visible on ultra-thin sections stained with Ur-Pb. This led to the conclusion that the FCs are discrete entities. The body of the above data confirm here that each nucleolonema is fixed by its base to an interphase NOR-bearing chromosome from which it is a lateral extension.

The nucleolonemata probably contain the ribosomal genes since, during early germination, each of them comes from the stretching out and the intrusion within the nucleolus of the two peripheral knobs in which in situ hybridization has disclosed the presence of all the rDNA. These peripheral knobs correspond to the NORs. The two NORs adjacent to the nucleolar periphery observed in quiescent maize cells are still partially visible in the transcriptionally active nucleolus. They probably correspond to transcriptionally inactive rDNA of the heterochromatic segment of the interphase NOR not involved in the formation of the nucleolus (32,34,36,37). To our knowledge, this is the first time that in electron microscopy a very ordered spatial distribution of intranucleolar chromatin is described in situ in a particular nucleolar subcomponent, the FCs. As previously shown (9), the FCs of maize and *Sinapis* nucleoli are small entities (between 0.22–0.58 μm in diameter), although the transcription units of these two species measure respectively 1.7 and 1.9 μm. Moreover, the transcriptionally active ribosomal genes in one nucleolus could number several hundred (34). This means that the rDNA should be highly compacted in the FCs. In animal cells, Tröster et al. (49) have observed that these genes are compacted by a factor of 4.

Since we have observed arborescent nucleolonemata which sometimes present loops in two evolutionary distant plant embryos, we can propose that the nucleolonematal organization is general for higher plants.

Acknowledgments

We thank Dr G. Feix (Institut für Biologie III der Universität, Freiburg, Germany) for the pMrl plasmid and Ms M. Dejace for patiently typing the various successive versions of this manuscript. We also thank Ms F. Motte-Tollet and Mr Gerstmans (Dept. of Chemistry, University of Liège, Belgium) for help in the preparation of the osmium ammine-B complex.

Literature Cited

1. Anteunis M, Pouchelet M, Gansmuller A, Robineaux R: The spatial organization of nucleolar DNA in phytohemagglutinin-stimulated lymphocytes of the guinea pig. Cell Tissue Res 235:65, 1984
2. Arroua ML, Hartung M, Devictor M. Berge-Lefranc JL, Stahl A: Localisation of ribosomal genes by in situ hybridization in the fibrillar centre of the nucleolus in the human spermatocyte. Biol Cell 44:337, 1982
3. Bateman E, Paule MR: Promoter occlusion during ribosomal RNA transcription. Cell 54:985, 1988
4. Benavente R, Reimer G, Rose KM, Hügle-Dörr B, Scheer U: Nucleolar changes after microinjection of antibodies to RNA polymerase I into the nucleus of mammalian cells. Chromosoma 97:115, 1988
5. Benavente R, Rose KM, Reimer G, Hügle-Dörr B, Scheer U: Inhibition of nucleolar reformation after microinjection of antibodies to RNA polymerase I into mitotic cells. J Cell Biol 105:1483, 1987
6. Carlemalm E, Garavito RM, Villiger W: Resin development for electron microscopy and an analysis of embedding at low temperature. J Microsc 126:123, 1982
7. Cassidy BG, Yang-Yen H-F, Rothblum LI: Additional RNA polymer-

ase I initiation site within the nontranscribed spacer region of the rat rRNA gene. Mol Cell Biol 7:2388, 1987

8. Comings DE: Arrangement of chromatin in the nucleus. Hum Genet 53:131, 1980
9. Deltour R, Mosen H: Proposals for the macromolecular organization of the higher plant nucleolonema. Biol Cell 60:75, 1987
10. Deltour R, Mosen H, Bronchart R: Three-dimensional electron microscopy of the internal nucleolus-associated chromatin and of the nucleolar vacuoles during early germination of Sinapis alba. J Cell Sci 82:53, 1986
11. Deltour R, Motte P: The nucleolonema of plant and animal cells: a comparison. Biol Cell 68:5, 1990
12. Derenzini M, Farabegoli F: Selective staining of nucleic acids by osmium-ammine complex in thin sections from Lowicryl-embedded samples. J Histochem Cytochem 38:1495, 1990
13. Derenzini M, Hernandez-Verdun D, Farabegoli F, Pession A, Novello F: Structure of ribosomal genes of mammalian cells in situ. Chromosoma 95:63, 1987
14. De Winter RFJ, Moss T: The ribosomal spacer in Xenopus laevis is transcribed as part of the primary ribosomal RNA. Nucleic Acids Res 14:6041, 1986
15. Dupuy-Coin AM, Pébusque MJ, Seïte R, Bouteille M: Localization of transcription in nucleoli of rat sympathetic neurons. A quantitative ultrastructural autoradiography study. J Submicrosc Cytol 18:21, 1986
16. Ghosh S, Lettré R, Ghosh I: On the decomposition on the nucleolus with special reference to its filamentous structure. Z Zellforsch 101:254, 1969
17. Goessens G: Nucleolar structure. Int Rev Cytol 87:107, 1984
18. Granick D: Nucleolar necklaces in chick embryo fibroblast cells. II. Microscope observations of the effect of adenosine analogues on nucleolar necklace formation. J Cell Biol 65:418, 1975
19. Granick S, Granick D: Nucleolar necklaces in chick embryo myoblasts formed by lack of arginine. J Cell Biol 51:636, 1971
20. Harrington CA, Chikaraishi DM: Transcription of spacer sequences flanking the rat 45S ribosomal DNA gene. Mol Cell Biol 7:314, 1987
21. Hilliker AJ, Trusis-Coulter SN: Analysis of the functional significance of linkage group conservation in Drosophila. Genetics 117:233, 1987
22. Labhart P, Reeder RH: Characterization of three sites of RNA 3' end formation in the Xenopus ribosomal gene spacer. Cell 45:431, 1986
23. La Cour LF: The internal structure of nucleoli. In Darlington CD, Lewis KP, eds. Chromosomes today. London, Oliver and Boyd, 1966, 150
24. La Cour LF, Wells B: The loops and ultrastructure of the nucleolus of Ipheon uniflorum. Z Zellforsch 82:25, 1967
25. Lafontaine JG, Lord A: An ultrastructural and radioautographic investigation of the nucleolonemal component of plant interphase nucleoli. J Cell Sci 12:369, 1973
26. Lettré R, Siebs W, Paweletz N: Morphological observations on the nucleolus of cells in tissue culture with special regard to its composition. Natl Cancer Inst Monogr 23:107, 1966
27. Locke M, Leung H: Nucleolar necklace formation in response to hemolymph ecdysteroid peaks. Tissue Cell 17:589, 1985
28. Luck BT, Lafontaine JG: An ultracytochemical study of nucleolar organization in meristematic plant cells (Allium porrum). J Cell Sci 43:37, 1980
29. Manuelidis L: Indications of centromere movement during interphase and differentiation. Ann NY Acad Sci 450:205, 1985
30. Manuelidis L: Individual interphase chromosome domains revealed by in situ hybridization. Hum Genet 71:288, 1985
31. Miller OL Jr: The nucleolus, chromosomes, and visualization of genetic activity. J Cell Biol 91:15s, 1981
32. Motte P, Deltour R, Mosen H, Bronchart R: Three-dimensional electron microscopy of the nucleolus and nucleolus-associated chromatin (NAC) during early germination of Zea mays L. Biol Cell 62:65, 1988
33. Olins AL, Moyer BA, Kim SH, Allison DP: Synthesis of a more stable osmium ammine electron-dense DNA stain. J Histochem Cytochem 37:395, 1989
34. Phillips RL, McMullen MD, Enomoto S, Rubenstein I: Ribosomal DNA in maize. In Gustafson JP, Apels R, eds. Chromosome structure and function. New York, Plenum Publishing, 1988, 201
35. Ploton D, Beorchia A, Ménager M, Jeannesson P, Adnet JJ: The three-dimensional ultrastructure of interphasic and metaphasic nucleolar argyrophilic components studied with high-voltage electron microscopy in thick sections. Biol Cell 59:113, 1987
36. Rawlins DJ, Shaw PJ: Localization of ribosomal and telomeric DNA sequences in intact plant nuclei by in-situ hybridization and three-dimensional optical microscopy. J Microsc 157:83, 1990
37. Rawlins DJ, Shaw PJ: Three-dimensional organization of ribosomal DNA in interphase nuclei of Pisum sativum by in situ hybridization and optical tomography. Chromosoma 99:143, 1990
38. Scheer U, Benavente R: Functional and dynamic aspects of the mammalian nucleolus. BioEssays 12:14, 1990
39. Scheer U, Hügle B, Hazan R, Rose KM: Drug-induced dispersal of transcribed rRNA genes and transcriptional products: immunolocalization and silver staining of different nucleolar components in rat cells treated with 5,6-dichloro-β-D-ribofuranosylbenzimidazole. J Cell Biol 99:672, 1984
40. Scheer U, Messner K, Hazan R, Raska I, Hansmann P, Falk H, Spiess E, Franke W: High sensitivity immunolocalization of double- and single-stranded DNA by a monoclonal antibody. Eur J Cell Biol 43:358, 1987
41. Scheer U, Raska I: Immunocytochemical localization of RNA polymerase I in the fibrillar centers of nucleoli. In Stahl A, Luciani JM, Vagner-Capodano AM, eds. Chromosomes today. London, Allen & Unwin, 1987, 284
42. Scheer U, Rose KM: Localization of RNA polymerase I in interphasic cells and mitotic chromosomes by light and electron microscopic immunocytochemistry. Proc Natl Acad Sci USA 81:1431, 1984
43. Schwarzacher HG, Wachtler F: Nucleolus organizer regions and nucleoli: cytological findings. In Stahl A, Luciani JM, Vagner-Capodano AM, eds. Chromosomes today. London, Allen & Unwin, 1987, 253
44. Steitz JA, Berg C, Hendrick JP, La Branche-Chabot H, Metspalu A, Rinke J, Yario T: A 5S rRNA/L5 complex is a precursor to ribosome assembly in mammalian cells. J Cell Biol 106:545, 1988
45. Tautz D, Dover GA: Transcription of the tandem array of ribosomal DNA in Drosophila melanogaster does not terminate at any fixed point. EMBO J 5:1267, 1986
46. Thiry M, Scheer U, Goessens G: Localization of DNA within Ehrlich tumour cell nucleoli by immunoelectron microscopy. Biol Cell 63:27, 1988
47. Thiry M, Thiry-Blaise L: In situ hybridization at the electron microscope level: an improved method for precise localization of ribosomal DNA and RNA. Eur J Cell Biol 50:235, 1989
48. Toloczycki C, Feix G: Occurrence of 9 homologous repeat units in the external spacer region of a nuclear maize rRNA gene unit. Nucleic Acids Res 14:4969, 1986
49. Tröster H, Spring H, Meissner B, Shultz P, Oudet P, Trendelenburg MF: Structural organization of an active, chromosomal nucleolar organizer region (NOR) identified by light microscopy, and subsequent STEM electron microscopy. Chromosoma 91:151, 1985
50. Van de Walle C, Bernier G, Deltour R, Bronchart R: Sequence of reactivation of ribonucleic acid synthesis during early germination of the maize embryo. Plant Physiol 157:632, 1976
51. Wachtler F, Mosgöller W, Schwarzacher HG: Electron microscopic in situ hybridization and autoradiography: localization and transcription of rDNA in human lymphocyte nucleoli. Exp Cell Res 187:346, 1990

Cancer Genet Cytogenet. **2003 Dec;147(2):134-9.** **Links**

Insertion (21;8)(q22;q22q22): a masked t(8;21) in a patient with acute myelocytic leukemia.

Onozawa M,
Fukuhara T,
Nigo M,
Takeda A,
Takahata M,
Yamamoto Y,
Miyake T,
Kanda M,
Maekawa I.

Department of Internal Medicine, Asahikawa City Hospital 1-65, Kinseicho 1 chome, Asahikawa, Hokkaido, Japan. masahiro.onozawa@nifty.ne.jp

A 43-year-old man was diagnosed with acute myelocytic leukemia with cellular maturation (AML-M2, according to the French-American-British classification criteria). A cytogenetic study with a G-banding method initially reported the karyotype as 45,X,-Y; however, dual-color, dual-fusion fluorescence in situ hybridization (FISH) with probes for the AML1 and the ETO genes showed an unusual pattern of signals, presenting one fusion signal on chromosome 21. Molecular study by reverse transcriptase polymerase chain reaction revealed the presence of a typical AML1/ETO chimeric gene. FISH with whole-chromosome painting probes targeting chromosomes 8 and 21 revealed insertion of part of 8 chromosome into the long arm of chromosome 21. We concluded that complicated translocations involving chromosomes 8 and 21 in this patient resulted in the development of the chimeric gene, AML1/ETO, on the long arm of chromosome 21. This aberrant location of AML1/ETO gene and the final karyotype of 45,X,-Y,ins(21;8)(q22;q22q22) could not be determined without molecular analysis. This abnormality is considered a masked t(8;21).

JOURNAL OF CLINICAL MICROBIOLOGY, June 1997, p. 1589–1591 Vol. 35, No. 6
0095-1137/97/$04.00+0

Detection of *Pneumocystis carinii* in Respiratory Specimens by PCR–Solution Hybridization Enzyme-Linked Immunoassay

ELENA ORTONA,[1] PAOLA MARGUTTI,[1] ENRICA TAMBURRINI,[2] PAOLA MENCARINI,[2] ELENA VISCONTI,[2] MARIA ZOLFO,[2] AND ALESSANDRA SIRACUSANO[1]*

Department of Immunology, Istituto Superiore di Sanità,[1] and Department of Infectious Disease, Università Cattolica del S. Cuore,[2] Rome, Italy

Received 17 July 1996/Returned for modification 12 November 1996/Accepted 25 February 1997

By using a recently developed PCR–solution hybridization enzyme-linked assay (PCR-SHELA), we investigated *Pneumocystis carinii* in bronchoalveolar lavage fluid samples and induced sputa of patients with pneumocystosis. In detecting *P. carinii*, PCR-SHELA proved more sensitive than immunofluorescence staining or a single PCR and significantly more diagnostically specific than a nested PCR. Our data suggest that PCR-SHELA could be used to detect *P. carinii* organisms in respiratory samples, particularly in patients with uncertain diagnoses.

PCR plus hybridization, especially nested or heminested PCR, has considerably increased the sensitivity of diagnostic tests for *Pneumocystis carinii* pneumonia (PCP) in respiratory specimens (4, 7, 8, 12). Several investigators have described the use of a PCR-based assay, consisting of detection of PCR products by an enzyme immunoassay (EIA) for the diagnosis of infectious diseases (3, 13). Recently, Cartwright et al. (1) have used a PCR-EIA to detect *P. carinii* in respiratory samples. Continuing our program of research into the molecular diagnosis of PCP, we assessed the ability of a new PCR–solution hybridization enzyme-linked assay (PCR-SHELA) to detect *P. carinii* in bronchoalveolar lavage fluid and induced sputum of human immunodeficiency virus (HIV)-infected patients suspected of having PCP.

Fifty-nine bronchoalveolar lavage and 66 induced sputum samples were obtained from 125 HIV-infected patients (91 men, 34 women; age range, 24 to 61 years) at the Department of Infectious Disease, Catholic University, Rome, Italy. All patients had no previous history of PCP. Patients underwent bronchoalveolar lavage for acute respiratory illness (fever, cough, shortness of breath) with abnormal chest signs and/or arterial hypoxemia and/or chest X-ray abnormalities, for unexplained pyrexia, or for suspected malignancies. Bronchoalveolar lavage was performed before starting high-dose anti-*P. carinii* therapy by two operators using the same multiple-lobe sampling technique. Sputum was induced by trained respiratory technicians using a protocol described by Ng et al. (5). Specimens were immediately processed and examined blindly, some aliquots were cultured in accordance with standard procedures to detect other pathogens.

The presence of *P. carinii* was tested by morphological staining and DNA detection by PCR. Immunofluorescence staining was performed with a commercial kit with monoclonal antibodies specific for cyst wall antigens (Monofluokit *P. carinii*; Diagnostic Pasteur, Paris, France). Immunofluorescence tests were considered positive if five or more cysts were detected on a smear.

Before PCR, bronchoalveolar lavage and induced sputum specimens were digested for 2 h at 55°C with proteinase K (final concentration, 0.5 mg/ml; Sigma). A PCR amplifying a portion of mitochondrial large-subunit rRNA was used with specific primers (11). In brief, pAZ102-E (5′-GATGGCTGT TTCCAAGCCCA-3′) and pAZ102-H (5′-GTGTACGTTGC AAAGTACTC-3′) (12) were used as outer primers for the first amplification round (mt-LSU single PCR) in a reaction volume of 25 μl containing 10 mM Tris-HCl (pH 8.3), 50 mM KCl, 3.0 mM $MgCl_2$, 0.2 mM each deoxynucleoside triphosphate, 1 mM each primer, and 2.5 U of *Taq* polymerase (Amplitaq; Perkin-Elmer). A hot-start technique was used. One microliter of the first amplification product was reamplified in a second reaction buffer (25 μl) containing the internal primer pair pAZ102-X (5′-GTGAAATACAAATCGGACTAGG-3′) and pAZ102-Y (5′-TCACTTAATATTAATTGGGGAGC-3′) (mt-LSU nested PCR) (9, 11). The two amplification products (346 and 263 bp) were visualized by ethidium bromide staining after agarose gel electrophoresis.

For PCR-SHELA, pAZ102-E and pAZ102-H labeled at the 5′ end with digoxigenin were used as primers in the amplification round and pAZ102-L2 (5′-CCAGCTATATCCTAGTC CGA-3′) (12) labeled at the 5′ end with biotin, used as the probe for hybridization, were added at the same time after the beginning of the reaction. Although the 5′ biotin-labeled pAZ102-L2 probe was present throughout PCR, it could not take part in the amplification reaction because a 3′ tail of dTTP mismatched with the corresponding sequence, thereby preventing oligonucleotide extension. The high annealing temperature also prevented the pAZ102-L2 probe from binding to its target sequence. After the PCR, the amplification products were denatured for 20 min at 99°C and the temperature was then lowered to 48°C to allow pAZ102-L2 to anneal to its complementary product sequence. We used a hot-start technique, and the PCR included 1 cycle of 94°C for 7 min, followed by 30 cycles of 94°C for 1.5 min, 55°C for 1.5 min, and 72°C for 1 min; after a denaturation cycle at 99°C for 20 min, the final hybridization was performed at 48°C for 90 min. Ten picomoles of each primer (pAZ102-E and pAZ102-H) was used in a 25-μl reaction volume. Hybridization of the amplification products with various pAZ102-L2 concentrations showed that 0.1 pmol was the optimum concentration for avoidance of background signals. The PCR buffer was the same as that used in the PCR. After amplification and hybridization, the PCR products were diluted by adding 200 μl of phosphate-buffered saline (PBS)–0.05% Tween 20 in ice.

* Corresponding author. Mailing address: Department of Immunology, Istituto Superiore di Sanità, Viale Regina Elena, 299, 00161 Rome, Italy. Phone: 39-6-49902760. Fax: 39-6-4440067.

Streptavidin-coated microtiter plates (Boehringer Mannheim, Indianapolis, Ind.) were blocked with sonicated salmon sperm DNA (Sigma Chemical Co., St. Louis, Mo.) for 20 min at room temperature. Wells were washed twice with PBS–0.05% Tween 20, a 100-μl volume of the diluted PCR products was added to each well, and the plate was incubated for 60 min at room temperature. One hundred microliters of peroxidase-conjugated anti-digoxigenin antibody (Boehringer Mannheim) per well diluted 1:500 in PBS–0.05% Tween 20 was added after four washings. After a 60-min incubation at room temperature and four washings, 100 μl of tetramethylbenzidine (Boehringer Mannheim) was added as the substrate; 10 min later, the reaction was stopped by adding 50 μl of 1 M H_2SO_4; and the A_{450} was measured. Each experiment included as positive controls standard end-point dilutions prepared with bronchoalveolar lavage fluid from a PCP patient (4.32×10^6 *P. carinii* nuclei/ml). PCR-SHELA permitted detection of four *P. carinii* nuclei/μl with a reproducible absorbance value of >0.490 (cutoff). PCP was diagnosed on the basis of identification of *P. carinii* organisms by morphological stains, detection of *P. carinii* DNA by a single PCR in respiratory specimens or lung tissue, and/or clinical findings and therapeutic response. Moreover, if the nested PCR was positive, PCP was diagnosed in patients with clinical suspicion in the absence of an alternative diagnosis, in particular, in those on specific prophylaxis. PCP was excluded when (i) the morphological examination of the bronchoalveolar lavage (not only the induced sputum) sample was negative, (ii) an alternative diagnosis was absent, (iii) resolution of the clinical and radiological picture occurred without anti-*P. carinii* therapy, and (iv) clinical PCP did not occur in a follow-up for at least 12 months. On the basis of the above criteria, 35 patients were considered to have PCP. In 32 cases, *P. carinii* organisms were identified in respiratory specimens (17 bronchoalveolar lavage fluid and 15 induced sputum samples). Three patients were classified as having PCP despite negative immunofluorescence staining and single PCR results obtained with their bronchoalveolar lavage fluid. In one of the three patients, who died 2 weeks later, *P. carinii* was identified in a lung examination. The other two patients were taking primary anti-*P. carinii* prophylaxis (one dapsone-pyrimethamine and the other aerosolized pentamidine).

Ninety patients were PCP negative but had the following respiratory diagnoses: pneumonia caused by *Pseudomonas* (16 cases) or *Staphylococcus* (3 cases) organisms, by *Streptococcus pneumoniae* (5 cases), by *Klebsiella pneumoniae* (7 cases), by mycobacteria (24 cases), or by *Aspergillus* (2 cases) or *Cryptococcus* (2 cases) organisms and Kaposi's sarcoma with lung involvement (5 cases). Twenty-six patients had neither opportunistic pathogens nor neoplasia.

Sensitivity, specificity, positive and negative predictive values calculated with a two-by-two table, and 95% confidence intervals were determined. Fisher's exact test (one sided) was used to determine the significance of differences between the sensitivity and specificity of the four diagnostic techniques. *P* values of ≤0.05 were considered to indicate statistical significance.

PCR-SHELA detected *P. carinii* DNA in all 20 bronchoalveolar lavage and 15 induced sputum specimens from patients with PCP at optical densities ranging from >0.55 to 2.7. Bronchoalveolar lavage fluid and sputum samples had similar mean optical densities (Fig. 1). A comparison of the results obtained by immunofluorescence, PCR, and PCR-SHELA with the 35 samples showed that PCR-SHELA and the nested PCR were more sensitive than immunofluorescence staining and the single PCR. In fact, all of the samples were positive by these two techniques, whereas only 32 of the 35 samples were positive by

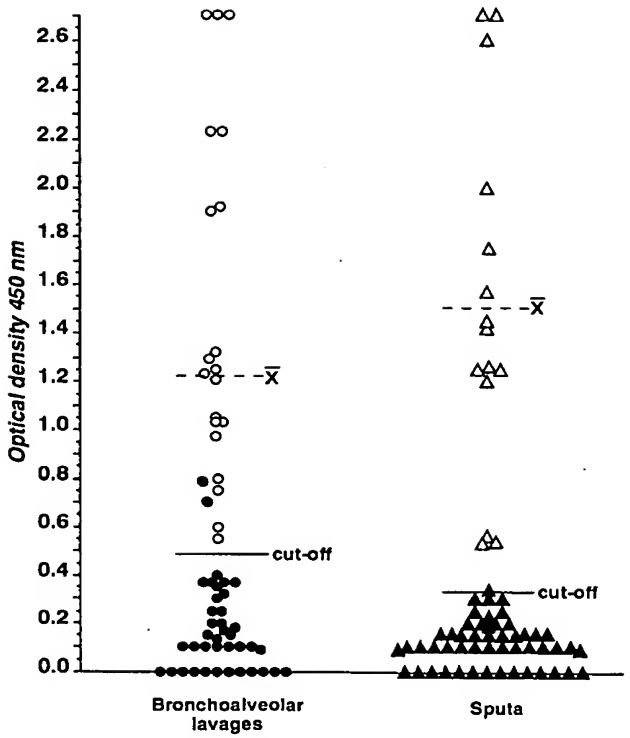

FIG. 1. Distribution of individual results obtained by PCR-SHELA with 59 bronchoalveolar lavage fluid and 66 induced sputum samples from patients with (open symbols) or without (solid symbols) pneumocystosis. The mean optical density of PCP-negative samples plus 2 standard deviations was taken as the cutoff level for positivity. ×, mean optical density of PCP-positive samples. Each value is the result of at least three experiments.

immunofluorescence assay and the single PCR (95% confidence interval, 90.00 to 100.00 versus 76.94 to 98.20). Eight of 90 patients without PCP were positive by the nested PCR; 2 of these were positive by PCR-SHELA also. Therefore, immunofluorescence staining, the single PCR, and PCR-SHELA were significantly more specific in detecting *P. carinii* than was the nested PCR (100 versus 92%, $P = 0.003$, 95% confidence interval of 95.98 to 100 versus 83.23 to 96.08; 98 versus 92%, $P = 0.05$, 95% confidence interval of 92.20 to 99.73 versus 83.23 to 96.08). Immunofluorescence and the single PCR failed to identify *P. carinii* in three bronchoalveolar lavage specimens from patients with PCP. The nested PCR revealed *P. carinii* in eight bronchoalveolar lavage fluid samples from patients without PCP (Table 1). The specificity of PCR SHELA was confirmed by bronchoalveolar lavage specimens from 20 HIV-negative, nonimmunosuppressed patients who underwent bronchoscopy for suspected, but not confirmed, lung neoplasia. These specimens were negative by all tests (data not shown).

To offer immunocompromised patients a better outcome, an immediate need is to improve the sensitivity, specificity, and quickness of diagnostic tests for PCP. The currently used routine immunofluorescence staining test, based on direct morphological identification of the organisms in respiratory specimens, is less sensitive than PCR in recurrent episodes of PCP and in patients who experienced PCP on prophylaxis (10). PCR plus hybridization performed with selected primers and probes (2) appears to be sensitive and specific, yet the use of a

TABLE 1. Comparison of the diagnostic values of immunofluorescence testing, mt-LSU single and nested PCRs, and PCR-SHELA

Test	No. of samples positive/total				% Sensitivity	% Specificity	Predictive value (%)	
	PCP$^+$ BAL[a]	PCP$^+$ induced sputum	PCP$^-$ BAL	PCP$^-$ induced sputum			Positive	Negative
Immunofluorescence	17/20	15/15	0/39	0/51	91.4	100	100	97
Single PCR	17/20	15/15	0/39	0/51	91.4	100	100	97
Nested PCR	20/20	15/15	8/39	0/51	100	92	81	100
PCR-SHELA	20/20	15/15	2/39	0/51	100	98	95	100

[a] BAL, bronchoalveolar lavage.

radiolabeled probe limits its application in routine diagnostic protocols. Although a nested PCR overcomes these technical problems, it has another disadvantage. Its high sensitivity complicates clinical interpretation and makes it necessary to exclude other respiratory disorders and laboratory cross-contamination.

In this study designed to find a new means of diagnosing PCP, we used a rapid PCR-SHELA technique previously applied by Qiao et al. to detect the *Leishmania donovani* complex (6). We used the primers targeting the mt-LSU rRNA gene, which have the best diagnostic efficiency in our experience (2), and we included the hybridization step in the amplification program. This technique proved faster and simpler than the PCR-EIA described by Cartwright et al. (1). In accordance with their results, PCR-SHELA yielded a higher sensitivity than immunofluorescence staining and similar specificity with respiratory samples from patients with PCP. Our experiments designed to test the diagnostic efficiency of *P. carinii* detection by PCR-SHELA and single and nested PCRs, all targeting the mt-LSU rRNA gene, showed that PCR-SHELA was more sensitive than the mt-LSU single PCR and more specific than the mt-LSU nested PCR.

The mt-LSU nested PCR revealed *P. carinii* in 8 of the 90 patients without PCP. With bronchoalveolar lavage samples, this positivity could simply depend on "subclinical infection/carrier status," as has been observed in patients with HIV-related severe immunodeficiency (2, 4, 7). Our finding that two of these nested-PCR-positive samples were also PCR-SHELA positive makes cross-contamination unlikely. A more likely explanation is that the different sensitivities of the two methods (nested PCR, one nucleus per microliter; PCR-SHELA, four nuclei per microliter) led to different results with samples containing few organisms.

In conclusion, our data suggest that PCR-SHELA will be useful for detecting *P. carinii* organisms in respiratory samples. An etiological diagnosis may be crucial in the management of HIV patients with suspicion of PCP in the era of new alternative regimens. Moreover, a molecular technique may be useful for examining noninvasive samples such as induced sputum in outpatient settings and in patients with suspicion of PCP who are receiving specific prophylaxis. The higher specificity of PCR-SHELA than nested PCR allows us to suggest the use of PCR-SHELA for diagnosis of PCP in patients whose diagnoses remain uncertain.

This work was supported by a grant from the IX AIDS Project-Istituto Superiore di Sanità, 1996, n. 940-S.

REFERENCES

1. **Cartwright, C. P., N. A. Nelson, and V. J. Gill.** 1994. Development and evaluation of a rapid and simple procedure for detection of *Pneumocystis carinii* by PCR. J. Clin. Microbiol. **32**:1634–1638.
2. **De Luca, A., E. Tamburrini, E. Ortona, P. Mencarini, P. Margutti, A. Antinori, E. Visconti, and A. Siracusano.** 1995. Variable efficiency of three primer pairs for the diagnosis of *Pneumocystis carinii* pneumonia by polymerase chain reaction. Mol. Cell. Probes **9**:333–340.
3. **King, J. A., and J. K. Ball.** 1993. Detection of HIV-1 by digoxigenin-labelled PCR and microtitre plate solution hybridization assay and prevention of PCR carry-over by uracil-*N*-glycosylase. J. Virol. Methods **44**:67–76.
4. **Leigh, T. R., H. O. Kangro, B. G. Gazzard, D. J. Jeffries, and J. V. Collins.** 1993. DNA amplification by the polymerase chain reaction to detect subclinical *Pneumocystis carinii* colonization in HIV$^+$ and HIV$^-$ homosexuals with and without respiratory samples. Respir. Med. **87**:525–529.
5. **Ng, V. L., I. Gartner, L. A. Weymouth, C. D. Goodman, P. C. Hopwell, and W. K. Hadley.** 1989. The use of mucolysed induced sputum for the identification of pulmonary pathogens associated with human immunodeficiency virus infection. Arch. Pathol. Lab. Med. **113**:488–493.
6. **Qiao, Z., M. A. Miles, and S. M. Wilson.** 1995. Detection of parasites of the *Leishmania donovani*-complex by a polymerase chain reaction-solution hybridization enzyme-linked immunoassay (PCR-SHELA). Parasitology **110**: 269–275.
7. **Tamburrini, E., P. Mencarini, A. De Luca, G. Maiuro, G. Ventura, A. Antinori, A. Ammassari, E. Visconti, L. Ortona, A. Siracusano, E. Ortona, and G. Vicari.** 1993. Diagnosis of *Pneumocystis carinii* pneumonia: specificity and sensitivity of polymerase chain reaction in comparison with immunofluorescence in bronchoalveolar lavage specimens. J. Med. Microbiol. **38**:449–453.
8. **Tamburrini, E., P. Mencarini, A. De Luca, A. Antinori, E. Visconti, A. Ammassari, L. Ortona, E. Ortona, A. Siracusano, and G. Vicari.** 1993. Simple and rapid two-step polymerase chain reaction for diagnosis of *Pneumocystis carinii* infection. J. Clin. Microbiol. **31**:2788–2789.
9. **Tamburrini, E., P. Mencarini, E. Visconti, M. Zolfo, A. De Luca, A. Siracusano, E. Ortona, and A. E. Wakefield.** 1996. Detection of *Pneumocystis carinii* DNA in blood by PCR is not of value for diagnosis of *P. carinii* pneumonia. J. Clin. Microbiol. **34**:1586–1588.
10. **Tamburrini, E., P. Mencarini, E. Visconti, A. De Luca, M. Zolfo, A. Siracusano, E. Ortona, R. Murri, and A. Antinori.** 1996. Imbalance between *Pneumocystis carinii* cysts and trophozoites in bronchoalveolar lavage fluid from patients with pneumocystosis receiving prophylaxis. J. Med. Microbiol. **45**:146–148.
11. **Wakefield, A. E., F. J. Pixley, S. Banerji, K. Sinclair, R. F. Miller, E. R. Moxon, and J. M. Hopkin.** 1990. Amplification of mitochondrial ribosomal RNA sequences for *Pneumocystis carinii* DNA of rat and human origin. Mol. Biochem. Parasitol. **43**:69–76.
12. **Wakefield, A. E., F. J. Pixley, S. Banerji, K. Sinclair, R. F. Miller, E. R. Moxon, and J. M. Hopkin.** 1991. Detection of *Pneumocystis carinii* with DNA amplification. Lancet **336**:451–453.
13. **Wilson, S. M., R. McNerney, P. M. Nye, P. D. Godfrey-Faussett, N. G. Stoker, and A. Voller.** 1993. Progress towards a simplified polymerase chain reaction and its application to diagnosis of tuberculosis. J. Clin. Microbiol. **31**:776–782.

APPLIED AND ENVIRONMENTAL MICROBIOLOGY, Sept. 1985, p. 615–622
0099-2240/85/090615-08$02.00/0

Vol. 50, No. 3

Activity Stain for Rapid Characterization of Pectic Enzymes in Isoelectric Focusing and Sodium Dodecyl Sulfate-Polyacrylamide Gels†

J. L. RIED AND A. COLLMER*

Department of Botany, University of Maryland, College Park, Maryland 20742

Received 27 February 1985/Accepted 28 June 1985

A system was developed for the rapid characterization of microbial pectic enzyme complexes and then tested on *Erwinia chrysanthemi* and *Sclerotium rolfsii*. Pectic enzymes in minute samples of crude culture filtrates were resolved by ultrathin-layer polyacrylamide gel isoelectric focusing and sodium dodecyl sulfate-polyacrylamide gel electrophoresis and then assayed with an ultrathin pectate-agarose overlay stained with ruthenium red. The simple procedure can be completed within 30 min after isoelectric focusing, can detect extremely low levels of pectate lyase (6.4×10^{-6} μmol of product per min), and is sufficiently sensitive to determine the pectate lyase isozyme profile of a single bacterial colony with a diameter of 4 mm. Pectate lyases and polygalacturonases can be distinguished by altering buffer conditions in the overlays. The assay system revealed additional isozymes not resolved by classical techniques and generally corroborated the previously published isoelectric points and molecular weights of the pectate lyase isozymes and exo-poly-α-D-galacturonosidase produced by *E. chrysanthemi* and the endopolygalacturonase and exopolygalacturonase produced by *S. rolfsii*.

Pectic enzymes play an important role in the interactions of microorganisms with higher plants. Pectic polymers (chains of 1,4-linked-α-D-galacturonic acid and methoxylated derivatives) are major structural constituents of plant middle lamellae and primary cell walls (27, 36). Purified pectic enzymes have multiple effects on plant tissues, including: (i) maceration and killing of cells (1, 3, 34), (ii) elicitation of disease defense reactions (12, 23), and (iii) rendering of cell walls more susceptible to attack by other microbial polysaccharidases (4, 14). Besides having an apparently important but still incompletely understood role in the development of plant diseases and the biodegradation of plant materials, pectic enzymes have several commercial uses (7).

Analysis of microbial pectic enzyme complexes and their interaction with plant tissue is limited by the techniques available for resolving and identifying the individual components. Various techniques have been reported for detecting pectic enzymes in electrophoretic gels by introducing pectic polymers into the gel before (11, 33) or after (24) electrophoresis or by activity staining a paper print of the resolved proteins (13), but none has met wide acceptance. Thus, in most studies of the pectate lyase isozymes produced by soft-rot erwinias, the time-consuming technique of isoelectric focusing in sucrose gradient columns has been used (for examples, see references 15, 16, 19, 26, 29, and 30).

Höfelmann et al. (18) have reported an alternative approach to the detection of depolymerases in isoelectric focusing gels through the use of an ultrathin-layer substrate-agarose overlay bonded to a plastic support sheet, and Bertheau et al. (5) have recently reported the use of a similar technique to detect pectic enzymes and other depolymerases in nondenaturing gels. We have developed the substrate-agarose overlay technique into a generalized system for rapidly analyzing microbial pectic enzymes in isoelectric focusing and sodium dodecyl sulfate (SDS)-polyacrylamide gels. In this report, we have used the previously characterized extracellular pectic enzyme complexes of *Erwinia chrysanthemi* CUCPB (Cornell University Collection of Phytopathogenic Bacteria) 1237 (10, 15) and *Sclerotium rolfsii* isolate 14 (2) to demonstrate the ability of the assay system to determine the isoelectric points and molecular weights of pectic enzymes in minute samples of crude protein mixtures.

We have used portions of this assay system to analyze the pectate lyase isozyme profiles of *Escherichia coli* clones containing *Erwinia chrysanthemi* genes (9).

(A preliminary report of this procedure has been published [J. L. Ried and A. Collmer, Phytopathology 74:834, 1984].)

MATERIALS AND METHODS

Source, preparation, and assay of pectic enzyme samples. Concentrated, desalted proteins were prepared from culture supernatants of polygalacturonic acid-grown cultures of *Erwinia chrysanthemi* CUCPB 1237 as previously described (9). This strain is a spontaneous rifampin- and streptomycin-resistant derivative (8) of strain 307 characterized by Garibaldi and Bateman (16). Osmotic shock fluids (17) were also prepared for isoelectric focusing from two *Escherichia coli* clones harboring recombinant plasmids containing *Erwinia chrysanthemi* DNA (9). Alternatively, protein samples from recombinant bacteria were prepared for isoelectric focusing from single-colony supernatants. Colonies (diameter, 4 mm) of recombinant, pectolytic *Escherichia coli* clones, grown on LB (25), were suspended in 0.030 ml of Tris hydrochloride (pH 7.5) and centrifuged for 1 min at $12,000 \times g$. The supernatants were then applied to the surface of an isoelectric focusing gel. Extracellular proteins from *S. rolfsii* Sacc. isolate 14 grown on bean hypocotyls (2) were obtained from D. F. Bateman and C. H. Whalen. The lyophilized enzyme preparation was suspended in 50 mM Tris hydrochloride (pH 7.5) and diafiltered extensively against the same buffer with an immersible CX-10 membrane (Millipore Corp.).

Pectate lyase activity was determined by monitoring the

* Corresponding author.

† Scientific article no. A-4160, contribution no. 7145, of the Maryland Agricultural Experiment Station.

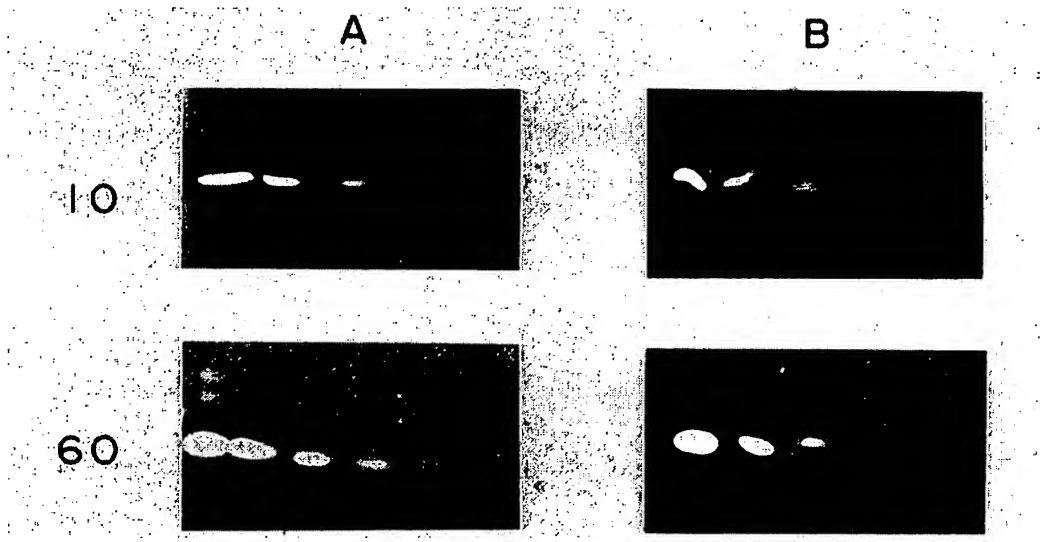

FIG. 1. The effect of overlay thickness on the sensitivity of the activity stain in detecting a pectate lyase isozyme in isoelectric focusing gels. Osmotic shock fluids from recombinant *Escherichia coli* clone CSR2 were resolved by ultrathin-layer isoelectric focusing and then incubated for either 10 or 60 min with 0.35-mm (A) or 0.8-mm (B) pectate-agarose overlays. Lanes in each panel received, from left to right, 4.0×10^{-3}, 8.0×10^{-4}, 1.6×10^{-4}, 3.2×10^{-5}, 6.4×10^{-6}, or 1.3×10^{-6} U of pectate lyase activity.

increase in A_{230} (32) of a reaction mixture containing 0.07% (wt/vol) polygalacturonic acid (product P21750 of Pfaltz and Bauer), 30 mM Tris hydrochloride (pH 8.5), 0.1 mM $CaCl_2$, and 1.7% (vol/vol) enzyme sample. Polygalacturonases were assayed by using the arsenomolybdate method of Nelson (28) to determine the increase in reducing groups in the reaction mixtures. For both types of enzymes, a unit of activity is defined as the amount of enzyme causing the formation of 1.0 μmol of product per min under optimal conditions at 25°C.

Preparation of ultrathin gels for isoelectric focusing and enzyme detection. Ultrathin (0.35-mm) polyacrylamide gels were cast for isoelectric focusing as described in the instructions of the manufacturer (FMC Corp.). Polyacrylamide solutions containing 5% acrylamide (Bio-Rad Laboratories), 0.17% *N,N'*-methylenebisacrylamide (Bethesda Research Laboratories), 20% (vol/vol) glycerol, 0.25 ml of Pharmalyte carrier ampholytes (pH 3 to 10; Pharmacia Fine Chemicals), 0.005 ml of *N,N,N',N'*-tetramethylenediamine (Bethesda Research Laboratories), and 0.019 ml of 10% ammonium persulfate per 5.0 ml of total volume were cast by capillary action between two glass plates separated by spacers. On one of these glass plates, a gel support film (100 by 125 mm) for acrylamide (Bio-Rad Laboratories) was affixed by a thin film of water. Polymerization occurred within 15 min.

Ultrathin (0.35-mm) pectate-agarose overlay gels for enzyme detection were cast as described above except that gel support film for agarose (Bio-Rad Laboratories) was used, the agarose solution was heated to 95°C, and the gel mold was heated to 50°C before casting. The agarose solution contained 1% agarose (Bethesda Research Laboratories), 0.1% polygalacturonic acid, and the following buffers designed for differential detection of particular pectic enzymes: for *Erwinia chrysanthemi* pectate lyase, 50 mM Tris hydrochloride (pH 8.5)–1.5 mM $CaCl_2$; for *Erwinia chrysanthemi* exo-poly-α-D-galacturonosidase, 100 mM potassium phosphate (pH 6.5)–10 mM EDTA; and for *S. rolfsii* exo- and endo-polygalacturonases, 50 mM potassium acetate (pH 4.5)–10 mM EDTA. Although thicknesses of 0.35 mm for polyacrylamide and agarose gels were optimum for conservation of electrofocusing reagents and for assay sensitivity, gels 0.8 mm thick were easier to cast and provided greater reproducibility.

Ultrathin-layer isoelectric focusing of proteins. Isoelectric focusing was performed at 6°C on an LKB 2117 Multiphor apparatus modified by the use of adjustable electrofocusing electrodes (Bio-Rad Laboratories). The ultrathin polyacrylamide gel was trimmed to remove 2 mm of gel from the edges of the support film and affixed to the cooling plate by means of a thin film of water. Excess water was removed from underneath the support film by absorbent paper before preelectrofocusing to minimize distortions in the pH gradient resulting from gel contact with water. Electrode wicks (Bio-Rad Laboratories) for the anode and cathode were soaked for several minutes in 0.04 M aspartic acid and 0.5 M NaOH, respectively, and the excess electrolyte was removed by absorbent paper. Enhanced resolution in the alkaline region of the isoelectric focusing gel was obtained when the cathodic wick was then saturated with a 2% Pharmalyte carrier ampholyte solution (pH 8 to 10.5) before application to the gel. Electrofocusing was performed in a 100% N_2 atmosphere maintained in a plastic, rectangular food storage container modified to house the cooling plate and electrodes. This increased the uniformity of the pH gradient across the gel by eliminating condensation on the gel surface and also reduced cathodic drift resulting from absorption of CO_2. The gel was preelectrofocused for 30 min at a constant 2.0 W. Protein samples of up to 15 μl were applied directly onto the gel as a series of drops in each lane or indirectly via a small tab of electrode strip paper (Bio-Rad Laboratories). Subsequent electrofocusing was for 60 min at a constant 4.5 W with a maximum of 2,000 V; sample application tabs were removed 15 min after electrophoresis was begun.

SDS-polyacrylamide gel electrophoresis and enzyme renaturation. SDS-polyacrylamide gel electrophoresis was

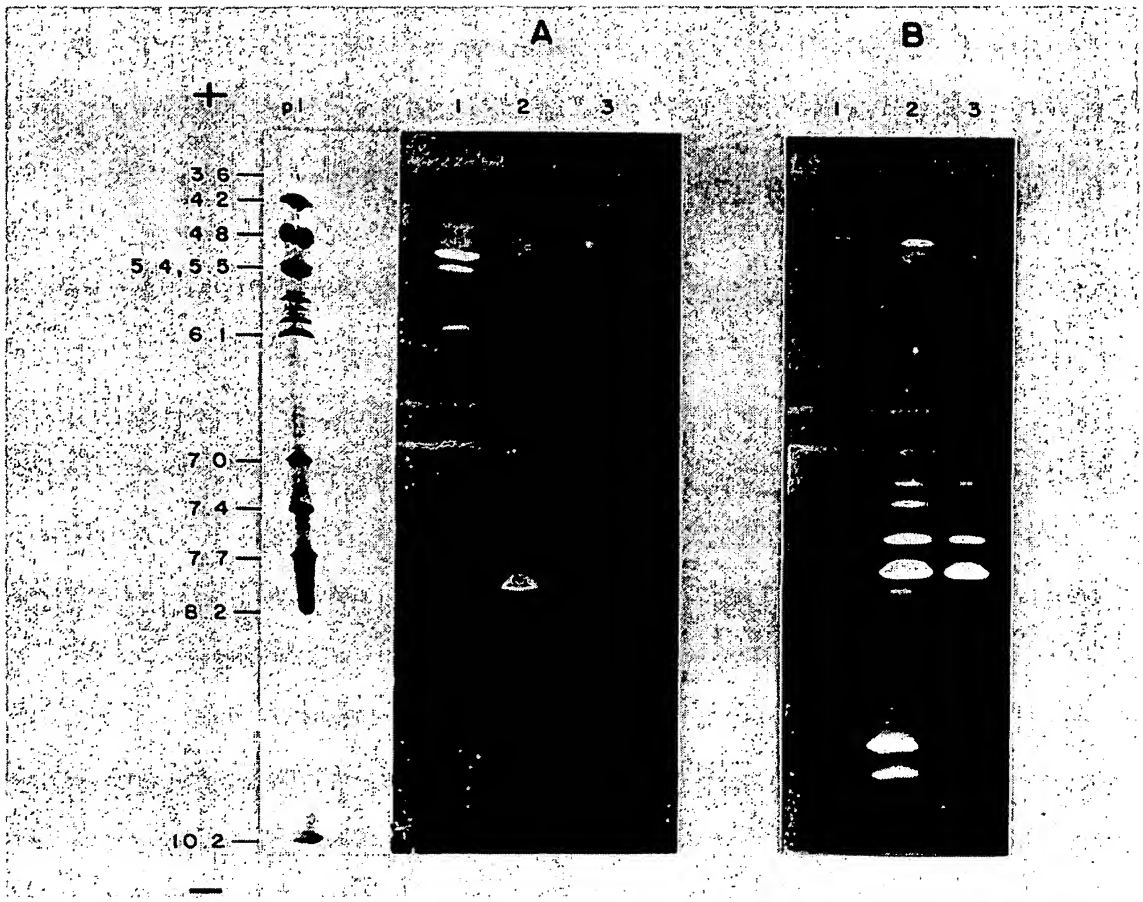

FIG. 2. Detection and differentiation of the pectic enzymes produced by *Erwinia chrysanthemi*, *S. rolfsii*, and recombinant *Escherichia coli* clone CSR50 after resolution by ultrathin-layer isoelectric focusing. Concentrated and desalted samples were electrophoresed on a single isoelectric focusing gel which was divided into three sections for processing. The lane containing pI markers (amyloglucosidase, glucose oxidase, ovalbumin, β-lactoglobulin, carbonic anhydrase, horse myoglobin minor and major bands, whale myoglobin minor and major bands, cytochrome *c*; FMC Corp.) was immediately stained for protein. The remaining lanes were incubated for 10 min with two diagnostically buffered pectate-agarose overlays. In panel A, overlays were buffered with 50 mM potassium acetate (pH 4.5) and 10 mM EDTA. In panel B, overlays were buffered with 50 mM Tris hydrochloride (pH 8.5) and 1.5 mM $CaCl_2$. Lane 1, *S. rolfsii*; lane 2, *Erwinia chrysanthemi*; lane 3, *Escherichia coli* clone CSR50.

performed by using the system of Laemmli (22) with a resolving gel containing 10% acrylamide, 0.33% bisacrylamide, and 20 μg of bovine serum albumin (Sigma) per ml to enhance renaturation of electrophoresed enzymes; the stacking gel contained 5% acrylamide–0.17% bisacrylamide. The SDS (Bio-Rad Laboratories) concentration was 0.1% in the gel and running buffer. Samples were held at 100°C for 2 min in sample buffer (2% SDS, 10% sucrose, 50 mM dithiothreitol [DTT], 125 mM Tris hydrochloride [pH 6.8], 0.003% bromphenol blue) before being cooled to 0°C. It was necessary to eliminate the DTT from the sample buffer for detection of depolymerizing activity from *S. rolfsii* protein samples. Samples were electrophoresed at 12.5 mA for 2.0 h through a 0.75-mm gel in a small, vertical slab unit (model SE 200; Hoefer Scientific Instruments). Gels that were activity stained for pectate lyase and exo-poly-α-D-galacturonosidase were incubated for 2 h with shaking in three 100-ml changes of 10 mM Tris hydrochloride (pH 7.5) (20). For *S. rolfsii* polygalacturonase detection, the gel was incubated with 10 mM potassium acetate (pH 4.5). Subsequently, these gels were protein stained by overnight immersion in a solution containing 0.1% (vol/vol) Coomassie brilliant blue R (Sigma), 10% (vol/vol) acetic acid, and 50% (vol/vol) methanol; the gels were destained in 10% acetic acid–50% methanol and then swelled to their original size in 10% acetic acid.

Activity stain overlay technique for detecting pectic enzymes after isoelectric focusing and SDS-polyacrylamide gel electrophoresis. Pectate-agarose overlays constructed as described above were placed directly onto the gel to be assayed. Air bubbles trapped between the two gels were removed by gently rubbing the plastic backing of the overlay with the tip of a rounded glass stirring rod. The sandwiched gels were incubated for various times in a moist chamber at room temperature for isoelectric focusing or at 30°C for SDS-polyacrylamide gel electrophoresis (the temperature of incubation was not critical), and then the overlays were immersed in 0.05% (wt/vol) ruthenium red (Sigma) for 20 min, rinsed in distilled water and preserved by drying at 50°C for 45 min. The overlays were then placed between clear

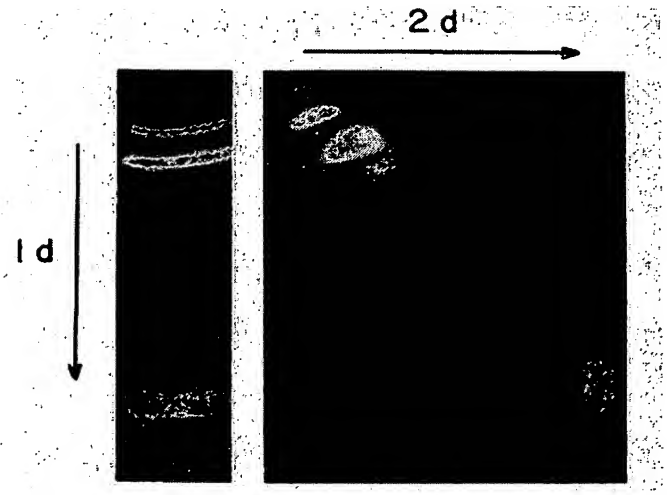

FIG. 3. Two-dimensional ultrathin-layer isoelectric focusing of the major *Erwinia chrysanthemi* pectate lyase isozymes. The first-dimension isoelectric focusing gel (ca. pH 7.0 to 10.0) was incubated for 10 min with a pectate-agarose overlay and then placed perpendicular to the pH gradient on a second ultrathin-layer isoelectric focusing gel. The electrofocused second dimension gel was then incubated with a pectate-agarose overlay for 15 min.

plastic sheets and photographed with a green filter (Wratten no. 58).

Detection of pectolytic bacterial colonies. We have applied the overlay technique to the detection of pectolytic *Escherichia coli* colonies which have been transformed by recombinant plasmids containing *Erwinia chrysanthemi* DNA (9). Putative pectolytic *Escherichia coli* cells were plated onto agar plates containing the appropriate antibiotics and incubated until colonies were about 2 mm in diameter. Whatman no. 1 filter paper was briefly laid onto each plate, removed (taking most of each colony), and then placed onto the agarose overlay. The resulting sandwich was covered with plastic wrap and incubated at 30°C for 30 to 60 min. The filter paper was then removed, and the overlay was vigorously

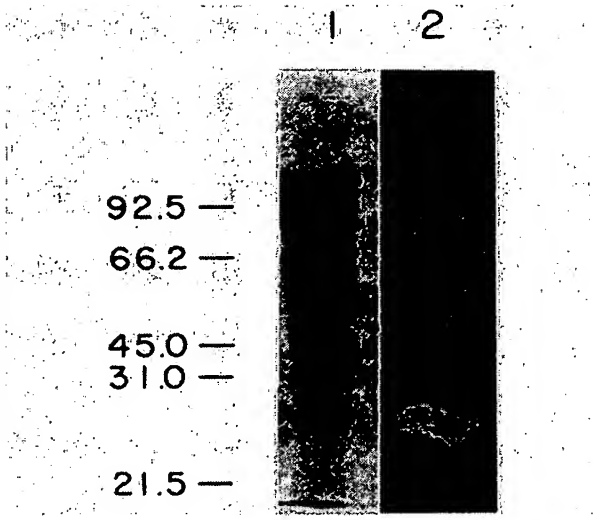

FIG. 5. Detection in SDS-polyacrylamide gels of the polygalacturonase and exopolygalacturonase produced by *S. rolfsii*. Gels were developed as described in the legend to Fig. 4 except that a 50 mM potassium acetate (pH 4.5)–10 mM EDTA buffer was used in the overlay. The sample contained 10.0 U of hydrolase, and the incubation with the pectate-agarose overlay was for 60 min. Lane 1, Coomassie-stained protein; lane 2, activity-stained overlay. The positions of molecular weight markers (described in the legend to Fig. 4) are shown at the left.

washed in running water to remove adhering bacteria and then stained in 0.05% ruthenium red.

RESULTS

Determination of the limit of sensitivity for detection of pectate lyase in ultrathin-layer isoelectric focusing gels. The sensitivity of the pectate-agarose overlay technique was determined with osmotic shock fluids from recombinant *Escherichia coli* clone CSR2 because this strain produces a single major pectate lyase isozyme. The gel was incubated with overlays of different thicknesses for different periods of

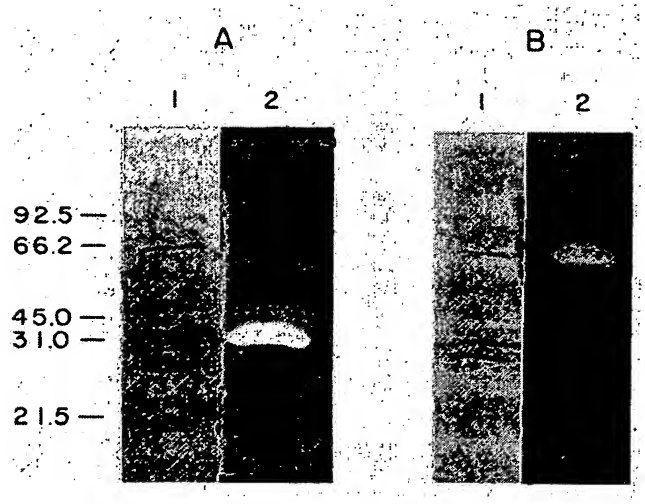

FIG. 4. Detection in SDS-polyacrylamide gels of the pectate lyase and exo-poly-α-D-galacturonosidase produced by *Erwinia chrysanthemi*. Both protein samples contained 1.6 U of pectate lyase and 0.19 U of exo-poly-α-D-galacturonosidase. Extracellular proteins of *Erwinia chrysanthemi* were resolved by SDS-polyacrylamide gel electrophoresis. The SDS was removed, and the gel was incubated at 30°C with a pectate-agarose overlay before protein staining. (A) Pectate lyase detection after 60 min of incubation with an overlay containing 50 mM Tris hydrochloride (pH 8.5) and 1.5 mM $CaCl_2$. Lane 1, Coomassie-stained protein; lane 2, activity-stained overlay. (B) Exo-poly-α-D-galacturonosidase detection after 120 min of incubation with a pectate-agarose overlay containing 100 mM potassium phosphate (pH 6.5) and 10 mM EDTA. Lane 1, Coomassie-stained protein; lane 2, activity-stained overlay. The positions and sizes (in thousands) of molecular weight markers (phosphorylase B, bovine serum albumin, ovalbumin, carbonic anhydrase, and soybean trypsin inhibitor; Bio-Rad Laboratories) are shown at the left. In our system, carbonic anhydrase (M_r, 31,000) migrated anomalously relative to the remaining standards. For this reason, this protein was not used in calculating the molecular weights of the unknown proteins.

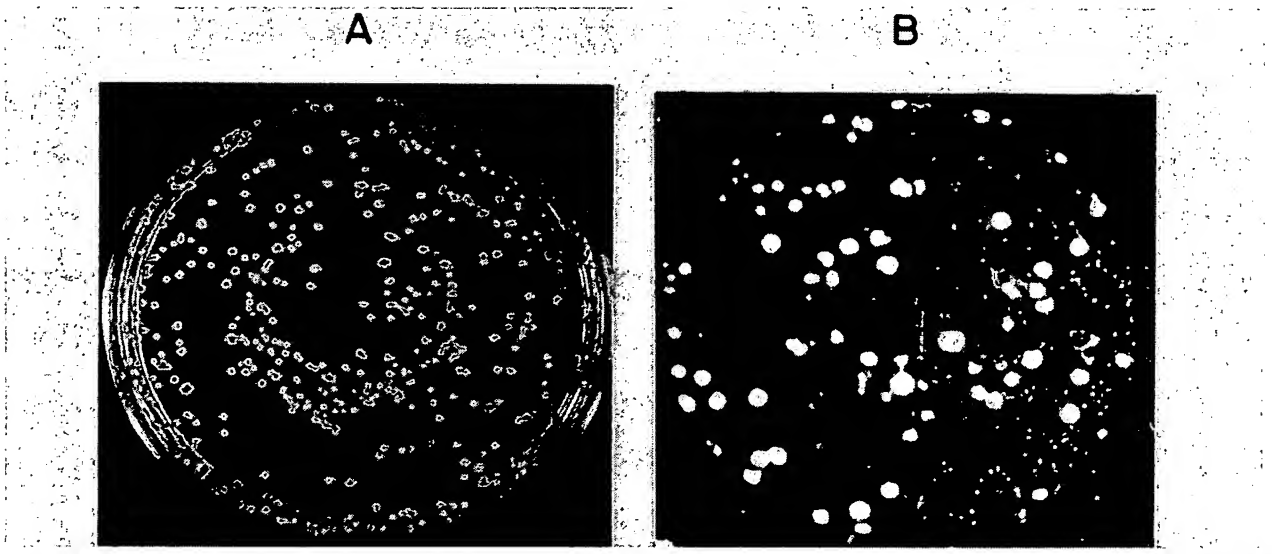

FIG. 6. Detection of pectolytic recombinant *Escherichia coli* clones in a background of 90% nonpectolytic *Escherichia coli*. (A) Colonies before assay; (B) agarose overlay of A.

time after isoelectric focusing of a dilution series of the osmotic shock fluid preparation (Fig. 1). The 0.35-mm agarose overlay was most sensitive, detecting 6.4×10^{-6} U of pectate lyase after 60 min of incubation and 3.2×10^{-5} U after 10 min (Fig. 1A). The 0.8-mm overlay detected only 1.5×10^{-4} U after both 10- and 60-min incubations (Fig. 1B). Overlays substantially less than 0.35 mm thick did not stain well. Resolution of pectate lyase isozymes diminished with increased sample activity and overlay incubation time (Fig. 1).

The sensitivity of the agarose overlay technique with SDS-polyacrylamide gels is about 0.10 U of pectate lyase after 60 min with 0.35-mm agarose gels (data not shown). This reduction in sensitivity compared with isoelectric focusing necessitates the use of a proportionately larger sample volume or an increased concentration of the enzyme.

Differential detection of polygalacturonic acid depolymerizing enzymes after isoelectric focusing. The composition of the agarose overlay can be varied to differentially detect pectate lyases (β-eliminative enzymes which have high pH optima and require a divalent cation) or polygalacturonases (hydrolytic enzymes which have acidic pH optima and are not inactivated by EDTA) (31). Figure 2 shows areas of pectolytic activity in identical sets of samples subjected to isoelectric focusing. In panel A, the overlay was buffered at pH 4.5 and contained 10.0 mM EDTA to optimize detection of *S. rolfsii* polygalacturonases and inhibit *Erwinia chrysanthemi* pectate lyases. Lane 1 shows three major bands of hydrolytic activity for *S. rolfsii* in the acidic area of the gel corresponding to pH's 5.1, 5.5, and 6.0. Lane 2 shows a single band of hydrolytic activity for *Erwinia chrysanthemi* at pH 8.0. In lane 3, a pectolytic *Escherichia coli* transformant previously testing negative for hydrolytic activity shows no depolymerase activity. In panel B, the same set and concentration of samples was focused, but the overlay had a pH of 8.5 and contained calcium. Under these conditions, the *S. rolfsii* polygalacturonases were completely inactive (lane 1), whereas the pectate lyases of both *Erwinia chrysanthemi* (lane 2) and the *Escherichia coli* transformant (lane 3) were active. The *Escherichia coli* transformant did not produce as many bands as *Erwinia chrysanthemi* apparently because not all of the pectolytic genes of *Erwinia chrysanthemi* were cloned. The faint band at pH 8.0 in lane 2, panel B, is probably the exo-poly-α-D-galacturonosidase of *Erwinia chrysanthemi* since it has the appropriate pI value and is not produced by the *Escherichia coli* transformant (Fig. 2A, lane 3).

Demonstration that the multiple isozymes of pectate lyase are not artifacts of isoelectric focusing. The basic portion of an isoelectric focusing gel of *Erwinia chrysanthemi* culture supernatants was subjected to isoelectric focusing in a second dimension (Fig. 3). Only a single band of activity was generated in the second dimension for each band resolved in the first dimension, indicating that the multiplicity of isozymes is not an artifact generated by isoelectric focusing. They arise from different structural genes or posttranslational modification or both.

Differential detection of pectate lyase and polygalacturonase after SDS-polyacrylamide gel electrophoresis. The pectate-agarose overlay technique detected renatured pectate lyase and polygalacturonase after SDS-polyacrylamide gel electrophoresis (Fig. 4 and 5). Pectate-agarose overlays revealed two major bands of activity corresponding to molecular weights of 36,000 and 44,000 for *Erwinia chrysanthemi* (Fig. 4A) and a single band of exo-poly-α-D-galacturonosidase activity (Fig. 4B). Not all of these enzymes renatured equally. The 44,000-molecular-weight band of activity required a threefold longer buffer wash after electrophoresis for enzyme detection than did the 36,000-molecular-weight band. For *S. rolfsii*, the overlay detected two bands of polygalacturonase activity corresponding to molecular weights of 52,000 and 29,000 (Fig. 5). The presence of DTT in the sample buffer prevented the detection of polygalacturonase, indicating the presence of essential disulfide linkages.

The use of isopropanol for renaturing enzymes after SDS-polyacrylamide gel electrophoresis has been reported to increase activity for certain enzymes (6). We found no increase in the sensitivity of the assay when isopropanol was used. In agreement with other workers (21), we found that

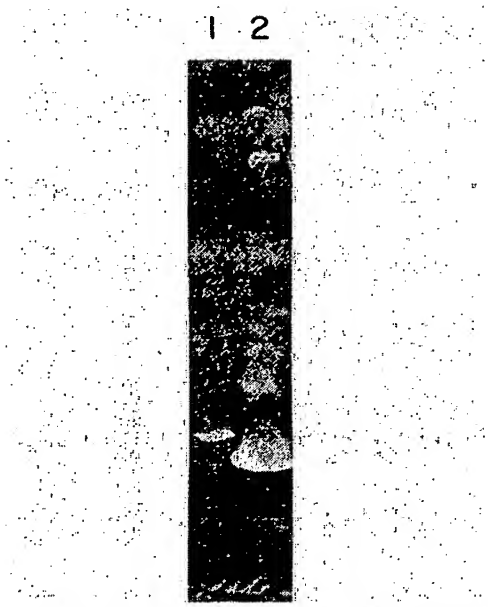

FIG. 7. Resolution of pectate lyase isozymes from single-colony supernatants. Samples (up to 15 μl) of single-colony supernatants (see the text for details) were electrophoresed on ultrathin isoelectric focusing gels, then assayed with a pectate-agarose overlay buffered with 50 mM Tris hydrochloride (pH 8.5)–1.5 mM $CaCl_2$. Lanes 1 and 2, pectolytic *Escherichia coli* clones producing two different isozymes of pectate lyase. The anode is at the top of the figure, and the cathode is at the bottom.

the source of SDS was critical for detecting enzymes; in this case, SDS from Sigma completely inhibited enzyme activity with or without DTT.

Detection of pectolytic bacterial colonies and resolution of pectic enzymes from single colony supernatants. The pectate-agarose overlay technique has been adapted for detecting pectolytic *Escherichia coli* colonies grown on standard microbiological media. After the filter paper was removed from the pectate-agarose overlay, vigorous rinsing of the overlay was required to remove bacteria that adhered to the surface; otherwise, these bacteria would prevent staining in that area. Pectolytic colonies produced a clear area (Fig. 6). Growth of the assayed colonies in the original petri plate, followed by proper alignment of the overlay with the petri plate, allowed pectolytic colonies to be identified and isolated from a background of nonpectolytic colonies.

A profile of the pectate lyase isozymes produced by *Escherichia coli* colonies could be obtained by suspending colonies grown on petri plates in buffer and subjecting the supernatant to isoelectric focusing (Fig. 7).

DISCUSSION

The combination of electrofocusing in ultrathin-layer polyacrylamide gels and SDS-polyacrylamide gel electrophoresis in small slab gels provides a rapid, high resolution method for analyzing a complex mixture of proteins. We have developed an activity-staining system for use in conjunction with these electrophoretic techniques which permits facile detection and preliminary characterization of pectic enzymes in crude protein mixtures. The detection technique is based on the ability of pectic enzymes diffusing from bands in a polyacrylamide gel to degrade the polygalacturonic acid in a diagnostically buffered, ultrathin pectate-agarose overlay and on the subsequent ability of ruthenium red to precipitate and stain (35) the surrounding, undegraded substrate.

This detection system provides a rapid means to determine pI profiles and molecular weights of polygalacturonic acid-degrading enzymes. Our results are summarized and compared with previously obtained values for *Erwinia chrysanthemi* and *S. rolfsii* in Tables 1 and 2. The pI values that we report corroborate and extend the enzyme complexity for each organism (Table 1). Significant differences are observed with SDS-polyacrylamide gel electrophoresis of the *Erwinia chrysanthemi* pectate lyase isozymes (Table 2). However, our values are in close agreement with those recently obtained for a different strain of *Erwinia chrysanthemi* by SDS-polyacrylamide gel electrophoresis of purified proteins (19). The polygalacturonase values from *S. rolfsii* that we report were obtained without DTT in the sample buffer because it prevented detection of enzyme activity. Nevertheless, the protein patterns appeared similar with or without DTT (data not shown), and our values are consistent with those previously reported (Table 2).

The activity staining system demonstrated with *E. chrysanthemi* and *S. rolfsii* pectic enzymes has at least four advantages over previously described methods. (i) Speed. Assay results are obtained in 30 to 80 min (depending on the desired sensitivity) after the completion of isoelectric focusing (Fig. 1) or 3 to 4 h after SDS-polyacrylamide gel electrophoresis, and each of the electrophoretic techniques is complete within 2 h. The activity-stained overlay can be immediately photographed or oven-dried for a permanent record. In the similar procedure of Bertheau et al. (5), a longer incubation of the substrate-agarose overlay with the isoelectrically focused gel (1 to 4 h versus 10 to 60 min) is recommended, as is a longer incubation of the overlay with the staining reagent (overnight in 1% cetyltrimethylammomium bromide versus 20 min in 0.05% ruthenium red).

(ii) Sensitivity. Figures 1 and 2 demonstrate the extreme sensitivity of the activity stain by showing its ability to detect an isoelectrically focused band containing only 6.4×10^{-6} U of pectate lyase activity (Fig. 1). Based on a specific

TABLE 1. Isoelectric points of major isozymes as determined by present and previous techniques

Enzyme	Isoelectric point of enzyme from:			
	Erwinia chrysanthemi		*S. rolfsii*	
	Present[a]	Previous	Present[a]	Previous
Pectate lyase	9.4 9.2 7.8 7.5	9.1,[b] 9.3[c] 7.9,[b] 8.3[c] 	—[d]	—
Exo-poly-α-D-galacturonosidase	8.0	8.3[c]	—	—
Polygalacturonases	—	—	5.1 5.5 6.0	5.2[e]

[a] Determined by activity-stained ultrathin-layer isoelectric focusing.
[b] Determined by sucrose gradient isoelectric focusing (15).
[c] Determined by granulated gel bed isoelectric focusing (10).
[d] —, Not detected in this organism.
[e] Determined by sucrose gradient isoelectric focusing (2).

TABLE 2. Molecular weights of enzymes as determined by present and previous techniques

Enzyme	Molecular weight of enzyme from:			
	Erwinia chrysanthemi		*S. rolfsii*	
	Present[a]	Previous	Present[a]	Previous
Pectate lyase	36,000 44,000	30,000–32,400[b]	—[c]	—
Exo-poly-α-D-galacturonosidase	68,000	67,000[d]	—	—
Polygalacturonases	—	—	29,000 52,000	28,000–31,000[e] 46,000–48,000[e]

[a] Determined by activity-stained SDS-polyacrylamide gel electrophoresis.
[b] Determined by gel filtration chromatography and sucrose density gradient centrifugation (15).
[c] —, Not detected in this organism.
[d] Determined by SDS-polyacrylamide gel electrophoresis of purified protein (10).
[e] Determined by gel filtration chromatography and sucrose density gradient centrifugation (2).

activity for pectate lyase of 300 U/mg of protein (1; Collmer and Whalen, unpublished results), this is equivalent to 20 pg of pectate lyase protein. This technique is sufficiently sensitive to determine the isozyme profile of single-colony supernatants (Fig. 7). This high sensitivity can be attributed to the low concentration (0.1%) of polygalacturonic acid, the intense differential staining by ruthenium red (35), and the thinness of the overlay (Fig. 1).

(iii) Resolution. The superior resolution achieved by activity-stained ultrathin-layer isoelectric focusing gels is shown by the clean separation of several isozymes of pectate lyase present in *Erwinia chrysanthemi* culture supernatants. These results, which corroborate those of Bertheau et al. (5), are in sharp contrast to earlier work with sucrose gradient isoelectric focusing, in which only two peaks of activity were reported (15, 16). The remarkable ability of pectate-agarose overlays to resolve closely spaced pectic enzymes, even when one band contains far more activity than another, can be attributed to the assay mechanism of detecting zones of enzymatic degradation in a background of relatively slowly diffusing substrate rather than detecting a diffusible product. High resolution is also favored by the rapidity of the assay (Fig. 1).

(iv) Adaptability. Because the substrate-containing overlay is separate from the polyacrylamide gel or other enzyme source to be assayed, the activity-staining system is adaptable to a wide variety of applications. We have demonstrated its usefulness for detecting pectolytic *Escherichia coli* colonies on petri plates (Fig. 6). In addition, alternate lanes of a single polyacrylamide gel can be assayed with overlay strips containing different buffers for the detection of different enzymes (Fig. 2, 4, and 5). Proteins remaining in the polyacrylamide gel can then be visualized with standard protein stains (Fig. 4 and 5) or electrophoresed in a second dimension (Fig. 3). We have used second-dimension isoelectric focusing of pectic enzymes after SDS-polyacrylamide gel electrophoresis to determine pI values for specific, pectolytic bands (9). These manipulations allow the rapid assignment of an isoelectric point and a molecular weight to each component of a pectic enzyme complex.

ACKNOWLEDGMENT

The work was supported by grant 84-CRCR-1-1366 from the Competitive Research Grants Office of the U. S. Department of Agriculture.

LITERATURE CITED

1. **Basham, H. G., and D. F. Bateman.** 1975. Killing of plant cells by pectic enzymes: the lack of direct injurious interaction between pectic enzymes or their soluble reaction products and plant cells. Phytopathology 65:141–153.
2. **Bateman, D. F.** 1972. The polygalacturonase complex produced by *Sclerotium rolfsii*. Physiol. Plant Pathol. 2:175–184.
3. **Bateman, D. F., and H. G. Basham.** 1976. Degradation of plant cell walls and membranes by microbial enzymes, p. 316–355. *In* R. Heitefuss and P. H. Williams (ed.), Encyclopedia of plant physiology, vol. 4. Physiological plant pathology. Springer-Verlag, Berlin.
4. **Bauer, W. D., K. W. Talmadge, K. Keegstra, and P. Albersheim.** 1973. The structure of plant cell walls. II. The hemicellulose of the walls of suspension-cultured sycamore cells. Plant Physiol. 51:174–187.
5. **Bertheau, Y., E. Madgidi-Hervan, A. Kotoujansky, C. Nguyen-The, T. Andro, and A. Coleno.** 1984. Detection of depolymerase isoenzymes after electrophoresis or electrofocusing, or in titration curves. Anal. Biochem. 139:383–389.
6. **Blank, A., R. H. Sugiyama, and C. A. Dekker.** 1982. Activity staining of nucleolytic enzymes after sodium dodecyl sulfate-polyacrylamide gel electrophoresis: use of aqueous isopropanol to remove detergent from gels. Anal. Biochem. 120:267–275.
7. **Chesson, A.** 1980. Maceration in relation to the post-harvest handling and processing of plant material. J. Appl. Bacteriol. 48:1–45.
8. **Collmer, A., and D. F. Bateman.** 1981. Impaired induction and self-catabolite repression of extracellular pectate lyase in *Erwinia chrysanthemi* mutants deficient in oligogalacturonide lyase. Proc. Natl. Acad. Sci. USA 78:3920–3924.
9. **Collmer, A., C. Schoedel, D. L. Roeder, J. L. Ried, and J. F. Rissler.** 1985. Molecular cloning in *Escherichia coli* of *Erwinia chrysanthemi* genes encoding multiple forms of pectate lyase. J. Bacteriol. 161:913–920.
10. **Collmer, A., C. H. Whalen, S. V. Beer, and D. F. Bateman.** 1982. An exo-poly-α-D-galacturonosidase implicated in the regulation of extracellular pectate lyase production in *Erwinia chrysanthemi*. J. Bacteriol. 149:626–634.
11. **Cruickshank, R. H., and G. C. Wade.** 1980. Detection of pectic enzymes in pectin-acrylamide gels. Anal. Biochem. 107:177–181.
12. **Davis, K. R., G. C. Lyon, A. G. Darvill, and P. Albersheim.** 1984. Host-pathogen interactions. XXV. Endopolygalacturonic acid lyase from *Erwinia carotovora* elicits phytoalexin accumulation by releasing plant cell wall fragments. Plant Physiol. 74:52–60.
13. **Drawert, F., and B. Krefft.** 1978. Charakterisierung extrazellularer Proteine und Enzyme aus Pektinkulturfiltraten von *Botrytis cinerea*. Phytochemistry 17:887–890.

14. **English, P. D., A. Maglothin, K. Keegstra, and P. Albersheim.** 1972. A cell wall degrading endopolygalacturonase secreted by *Colletotrichum lindemuthianum*. Plant Physiol. **49**:293–298.
15. **Garibaldi, A., and D. F. Bateman.** 1970. Association of pectolytic and cellulolytic enzymes with bacterial slow wilt of carnation caused by *Erwinia chrysanthemi* Burkh. McFad. et Dim. Phytopathol. Mediterr. **9**:136–144.
16. **Garibaldi, A., and D. F. Bateman.** 1971. Pectic enzymes produced by *Erwinia chrysanthemi* and their effects on plant tissue. Physiol. Plant Pathol. **1**:25–40.
17. **Heppel, L. A.** 1967. Selective release of enzymes from bacteria. Science **156**:1451–1455.
18. **Höfelmann, M., R. Kittsteiner-Eberle, and P. Schreier.** 1983. Ultrathin-layer agar gels: a novel print technique for ultrathin-layer isoelectric focusing of enzymes. Anal. Biochem. **128**: 217–222.
19. **Keen, N. T., D. Dahlbeck, B. Staskawicz, and W. Belser.** 1984. Molecular cloning of pectate lyase genes from *Erwinia chrysanthemi* and their expression in *Escherichia coli*. J. Bacteriol. **159**:825–831.
20. **Lacks, S. A., and S. S. Springhorn.** 1980. Renaturation of enzymes after polyacrylamide gel electrophoresis in the presence of sodium dodecyl sulfate. J. Biol. Chem. **255**:7467–7473.
21. **Lacks, S. A., S. S. Springhorn, and A. L. Rosenthal.** 1979. Effect of the composition of sodium dodecyl sulfate preparations on the renaturation of enzymes after polyacrylamide gel electrophoresis. Anal. Biochem. **100**:357–363.
22. **Laemmli, U. K.** 1970. Cleavage of structural proteins during the assembly of the head of bacteriophage T4. Nature (London) **227**:680–685.
23. **Lee, S.-C., and C. A. West.** 1981. Polygalacturonase from *Rhizopus stolonifer*, an elicitor of casbene synthase activity in castor bean (*Ricinus communis* L.) seedlings. Plant Physiol. **67**:633–639.
24. **Lisker, N., and N. Retig.** 1974. Detection of polygalacturonase and pectin lyase isoenzymes in polyacrylamide gels. J. Chromatogr. **96**:245–249.
25. **Maniatis, T., E. F. Fritsch, and J. Sambrook.** 1982. Molecular cloning: a laboratory manual. Cold Spring Harbor Laboratory, Cold Spring Harbor, N.Y.
26. **Mazzucchi, U., A. Alberghina, and A. Garibaldi.** 1974. Comparative immunological study of pectate lyases produced by soft-rot coliform bacteria. Phytopathol. Mediterr. **13**:27–35.
27. **McNeil, M., A. G. Darvill, S. C. Fry, and P. Albersheim.** 1984. Structure and function of the primary cell walls of plants. Annu. Rev. Biochem. **53**:625–663.
28. **Nelson, N.** 1944. A photometric adaptation of the Somogyi method for the determination of glucose. J. Biol. Chem. **153**:375–380.
29. **Pupillo, P., U. Mazzucchi, and G. Pierini.** 1976. Pectate lyase isozymes produced by *Erwinia chrysanthemi* Burkh. et al., in polypectate broth or in *Dieffenbachia* leaves. Physiol. Plant Pathol. **9**:113–120.
30. **Quantick, P., F. Cervone, and R. K. S. Wood.** 1983. Isoenzymes of a polygalacturonate *trans*-eliminase produced by *Erwinia atroseptica* in potato tissue and in liquid culture. Physiol. Plant Pathol. **22**:77–86.
31. **Rexová-Benková, L., and O. Markovič.** 1976. Pectic enzymes. Adv. Carbohydrate Chem. Biochem. **33**:323–385.
32. **Starr, M. P., and F. Moran.** 1962. Eliminative split of pectic substances by phytopathogenic soft-rot bacteria. Science **135**:920–921.
33. **Stegemann, H.** 1967. Enzym-elektrophorese in einschlusspolymerisaten des Acrylamids. B. Polygalakturonasen (pektinasen). Hoppe-Seyler's Z. Physiol. Chem. **348**:951–952.
34. **Stephens, G. J., and R. K. S. Wood.** 1975. Killing of protoplasts by soft-rot bacteria. Physiol. Plant Pathol. **5**:165–181.
35. **Sterling, C.** 1970. Crystal-structure of ruthenium red and stereochemistry of its pectic stain. Am. J. Bot. **57**:172–175.
36. **Talmadge, K. W., K. Keegstra, W. D. Bauer, and P. Albersheim.** 1973. The structure of plant cell walls. I. The macromolecular components of the walls of suspension-cultured sycamore cells with a detailed analysis of the pectic polysaccharides. Plant Physiol. **51**:158–173.

a·bove·men·tioned ☒(ə-bŭv′mĕn′shənd)

adj.

Mentioned previously.

n.

The one or ones mentioned previously.